

**Politecnico di Torino**

DIATI – Dipartimento di Ingegneria dell'Ambiente,  
del Territorio e delle Infrastrutture



Thesis

***“Laboratory analyses on artificial sand  
specimens”***

*Supervisor:*

Prof.ssa Verga Francesca

*Student:*

Di Giorgio Nicoletta

Academic year 2018/19

## Index

<b>Acknolegments</b> .....	<b>3</b>
<b>Introduction</b> .....	<b>4</b>
<b>1. A dive in the past history of a rock</b> .....	<b>5</b>
1.1 Where does a rock come from? .....	5
1.2 Core samples in Oil Field .....	6
<b>2. Manufacture of artificial cores</b> .....	<b>8</b>
2.1 Screening, Mixing, Moulding and Compaction .....	8
2.2 Particle Size Distribution Analysis.....	10
2.2.1 Laser Diffraction Method .....	10
2.2.2 Calculations.....	10
<b>3. Lab analyses on the created sand specimens</b> .....	<b>33</b>
3.1 Helium Porosimeter.....	33
3.2 Porosity measurements.....	35
3.3 Permeability measurements.....	36
3.4 Klinkenberg effect.....	43
3.5 VBA Coding Programming.....	45
3.6 The calculated permeability.....	46
3.7 Geometrical Considerations.....	47
<b>4. Correlation among properties of the core samples</b> .....	<b>62</b>
4.1 Grain size distribution vs Permeability .....	62
4.2 Grain size distribution vs Porosity .....	64
<b>Conclusion</b> .....	<b>67</b>
<b>References</b> .....	<b>68</b>

## *ACKNOLEGMENTS*

I offer my gratitude to the faculty of Petroleum and Natural Gas at the University of Miskolc, in Hungary, especially to the PhD student Adam Viktor Pasztor, who has supported me and helped me to perform this project work during the laboratory experiments.

A particular thanks, also, to my Italian supervisor, prof.ssa Francesca Verga, who has spent efforts on instructing me to study well, first, during the class lectures, and then, to guide me with the revision of this thesis.

Last but not least, the biggest dedication of this work to my family, who has played an important role in my education: without their unconditional support, I would not be here today.

## *INTRODUCTION*

The topic of this project work deals with the possibility to create artificial samples by means of a mixture of sand, cement and hydrate limestone, put together every time in a different proportions, to be tested in laboratories, avoiding the costly and long procedure of taking the real samples.

Another reason that justifies the makeup of those specimens is the number of cores you can retrieve from well drilling (usually a few); a virtually infinite number of specimens can be prepared in the lab and the dimensions of the cores can be decided according to the testing needs (there can be the need to perform specific analysis on very big samples, which are hard to get from the underground).

So, the idea is to show how the artificial sand specimens can easily substitute the real ones by using common sand, bought in a store, at a reasonable price and make all the necessary procedures to end up to a sample, which can be used for different kind of laboratory experiments.

The detailed description of the sand mixture investigation by means of laser scattering analysis and of the process applied to making up of 40 samples on which analyses of permeability and porosity were performed is provided. Each method used for the investigation will be explained, including the process, the tool used, the calculations and the obtained values. The porosity and permeability test results were then correlated to the grain size distribution, in order to understand the impact of the grain particles on the sample properties.

All the laboratory experiments were carried out at University of Miskolc, in Hungary, thanks to the help of a PhD student, Adam Viktor Pasztor.

## FIRST CHAPTER

### ***“A DIVE IN THE PAST HISTORY OF A ROCK”***

#### *1.1 Where does a rock come from?*

The discipline of geology, together with specialized studies of petrophysics, sedimentology, paleontology, stratigraphy and geochemistry, shows us the surrounded territory as a sequence of layers of different rock types that superimpose one upon the other by making the complex unit which is called Earth.

Thanks to those disciplines combined also with geophysics, it is possible to have an image of the subsurface. This fact, for sure influenced during the last decades the approach of reservoir engineers in the study of hydrocarbons exploration and production.

By definition a rock is an aggregate of minerals held together by chemical bonds, arranged in a proper manner, and subjected to several transformations which determine their subdivision in three main categories: igneous, sedimentary and metamorphic rocks (Selley, Richard C., *Applied Sedimentology*).

Igneous rocks derive from a process of cooling and solidification of a magma, coming from melted existing rocks present in the mantle and in the crust of our planet, by means of an increase in temperature, a decrease in pressure or a change in composition (Cipriani, Nicola -1996. *The encyclopedia of rocks and minerals*; Wikipedia source).

Sedimentary rocks form by processes of accumulation and deposition of sediments, which are subjected to several transformations (weathering, erosion, water and wind actions, and all the agents of denudation) and consequent cementation of particles onto the Earth's basin and ocean floors. These ones are the rocks which we are interested in because it's there where most frequently you can encounter hydrocarbon reserves (Cipriani, Nicola -1996. *The encyclopedia of rocks and minerals*; Wikipedia source).

Metamorphic rocks differ from the other two typologies, simply because their origin is due to chemical and physical transformations of existing rocks (protoliths) which change their forms according to the heat and the pressure at which they are subjected to.

The results of all these processes are then rocks which show particular properties such as chemical composition, permeability, porosity, particle size distribution, texture of the grains and so on, by which they are analyzed on purpose.

In details,

- *Chemical composition* refers to the crystalline structure of the inorganic solids that naturally formed a rock: the so called minerals, derived by a several combination of different elements (Oxygen, Silicon, Aluminum, Calcium, Magnesium, etc.);
- *Permeability* is defined as the ability of a porous rock, a sediment or a subsoil to transmit fluid through the pores present in the solid frame. How much permeable is a formation will give us the idea about the quantity of fluid that can be stored in (Encyclopedia.com, *Porosity and Permeability*; Ishimwe D., *Reservoir Rock Properties* );
- *Porosity* represents the void space in a rock that can be occupied by any fluids, such as water, oil or gas and it has a great importance in the oil field because it may evaluate the potential volume of hydrocarbon contained in a rock. It is also defined as the measure of the capacity of a rock to hold fluid (Ishimwe D., *Reservoir Rock Properties*);
- *Particle size distribution* is a way to characterize a rock based on the grains size and which gives the amount of particles present in relation with their size. It represents a powerful tool to interpret the geomorphic significance of the fluid dynamics and to classify especially clastic rocks;
- *Texture of the grains* is the orientation of the crystalline components in a sample, according to which we can distinguish a fine-grained rock, coarse-grained one and glassy based on the percentage of crystals present (Wikipedia);

Lots of other properties can be analyzed and mentioned in order to describe the complexity world behind a rock's formation. But for the purpose of this work, the above selected ones are considered sufficient for the analysis that has to be performed.

## 1.2 Core samples in Oil Field

In terms of Oil and Gas Industry more importance is given to the sedimentary rocks, which form typical structures in their basins, the well known "traps" made up of permeable layers (sandstone) where the valuable resources can be stored, and bounded by impermeable formations (for instance, shale). Because of this, sedimentary rocks acquires such an importance since are the most frequent places where to encounter hydrocarbons.

The main types can be distinguished among sandstones, shales, limestones, dolomites, and many, many others, but for sure sandstones are the most common (in fact, almost 60% of the worldwide reservoirs are made by them) (Selley, Richard C., *Applied Sedimentology*).

Most of the analysis performed in order to understand if a specific site shows the presence of possible hydrocarbon bearing levels are based on a first stage examination of core samplings.

Now, a successful analysis of the properties of a rock is made by a continuous steps in which it is relevant to define the most accurate procedure to follow. One of that is the sampling selection data from a core analysis.

A core is a sample of rock with a cylinder- like shape, 1 inch diameter and 3 inch length, thanks to which it is possible to have an insight into the main characteristics of a well: porosity, permeability, fluid saturation, grain density, all data that can help to have a better vision of the well conditions and its potential productivity.

Moreover, special core analysis can also involve measurements of wettability, capillary pressure and electrical characteristics to better investigate resistivity, cation-exchange-capacity, and formation volume factor.

In order to proceed with the core sampling, a long process has to be undertaken: starting from the drilling operations which are involved, to the selection of the cores (in fact, several types exist: full-diameter cores, oriented cores, sidewall cores, and native state cores) and not the least important the financial aspect in which has to put the investment of the project ([www.rigzone.com](http://www.rigzone.com), *How does core analysis work?*).

One innovative contribution is given by the fact that also in lab, cores can be reproduced by means of artificial processes, that lead to a creation of a realistic sample on which is possible to investigate whichever characteristics.

This possibility represents a good replacement for the real ones since not always the suitable core plugs are available or affordable, especially in terms of cost, but not only.

So, developing a technique in order to makeup artificial cores instead of using the real ones gives a great contribution particularly for practical reason and then for theoretical purpose.

Exactly this one will be the main task of this work, which will be based on the realization of artificial sand specimens on which perform experiments and EOR investigations.

## SECOND CHAPTER

### “MANUFACTURE OF ARTIFICIAL CORES”

#### 2.1 “Screening, Mixing, Moulding, and Compaction ”

In the creation of artificial cores the first process is the separation of sand particles, screening process, achieved in this case by using a sieve analysis (Jishun, *The Manufacture and Use of Artificial Consolidated Core Samples in China*).

This method allows to separate fine particles from the course ones and to determine the grain size distribution, by letting the material pass through sieves of progressively smaller mesh size.

The entire aggregate is then agitated, and the material whose diameter is smaller than the previous one passes through the sieve and collects into the other container below.

All the process is performed by several shakes, that can be done manually and/or mechanically, till the moment when all particles result separated in their range diameter.

Here, the used sieves are labelled by 800, 500, 315, 200 and below 200  $\mu\text{m}$ .

The results provided from the test are given by graphical form, in which is possible to see how each material is correlated to its size distribution.

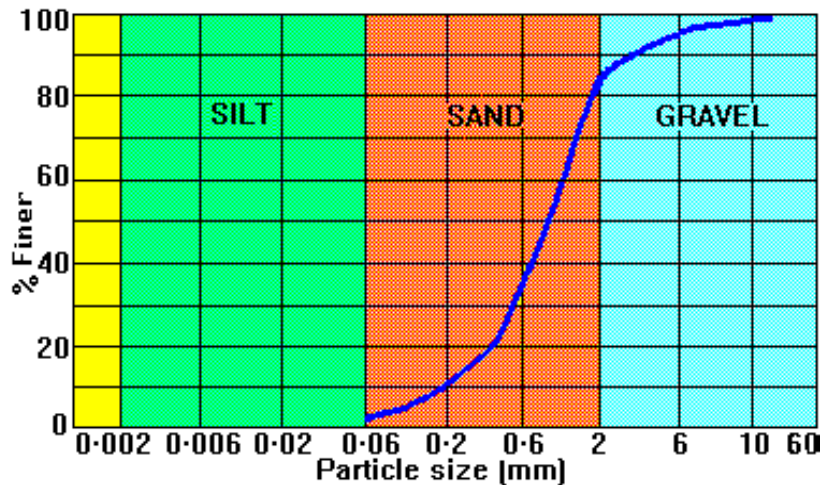


Figure 1- Particle Size Distribution, the Cumulative representation Curve (Google Imagine)

Then, one fraction of these components is taken to make the aggregate, mixed with hydrate limestone and cement according to an appropriate ratio to originate the first sample of the first series, A, up to the eighth one, H:

- 514 g sand
- 36 g hydrate limestone
- 50 g cement

After that, 100 g of the mixture are measured and put in a specimen made by steel, covered in with a plastic bandage. Then, the bottom is closed with a filter paper and the material can fulfil it. On the

top of the sample a plug is inserted and the core is ready to be compressed. This procedure is repeated for the next 4 cores, that are considered in the series.

The press works by torque, so one by one the core is compressed and then all together are watered for at least 4 hours.

Only later they are left drying about 12 hours. The following step is to put them under vacuum, under a pressure of 0.8 kp/cm<sup>2</sup>, for about 3-5 hours.

Finally, they can be taken out from the cylinders and drying 1 day before their usage.

Table 1- Mixture composition of specimen

Mixture Composition				
Series of 5 samples	sand 500	sand 315	sand 200	sand <200
A	50%	50%	x	x
B	30%	70%	x	x
C	x	x	50%	50%
D	x	50%	50%	x
E	x	50%	x	50%
F	70%	30%	x	x
G	25%	25%	25%	25%
H	75%	25%	x	x

Sadly, not all the cores could resist to the compression and the pressure. So, the majority broke up when they were taken out from the cylinder, others simply shown fractures that altered the parameters. Fortunately, a good number was preserved for the time available to make the core up, and it was sufficient to carry on the analysis of the project work.

## 2.2 Particles -Size Distribution (PSD) Analysis

With the term Particle Size Distribution of a granular material is meant the value or the mathematical function that can represent the amount of particles present according to their size (Wikipedia).

It is defined by the method used to determine it: several methods exist, in fact, for the determination of PSD. The most used is the sieve analysis, explained in 2.1, due to its ease, cost and simple interpretation.

But other measurements techniques can be applied, which use photoanalysis, optical method, electroresistant method, sedimentation technique, and also among them it is noticeable to remember the laser diffraction analysis, used in this work to get the mathematical function typical of each size range analyzed.

### 2.2.1 Laser Diffraction Method

This technique uses the diffracted light produced by a laser beam that passes through a dispersion of particles in air or in a liquid. It is more common for particle size which varies between 0,1 and 3000  $\mu\text{m}$ .

One advantage is its fast response, and easy applicability for small samples. Moreover, it can generate a continuous measurement for analyzing process streams (Mc Cave, I. N., *Evaluation of a Laser Diffraction Size Analyzer for Use with Natural Sediments*).

Laser diffraction measures PSD by determining the angular variation in intensity of light scattered as a laser beam through a particulate sample. The angle of diffraction increases as particle size decreases. So, large particles scatter light at small angles relative to the laser beam and small particles scatter light at large angles. This is known as the Fraunhofer diffraction theory.

The specific tool used in lab is the Laser Scattering LA-950V2, which gives results in terms of seconds and by means of a computer you can have an operator interface for instrument control, color graphics, and data management and retrieval. Thanks to that, particle size distributions for different range are available for the calculation of the PSD of the mixture we created.

Below, it is possible to see the table with the values obtained.

### 2.2.2 Calculations

The procedure follows this logic: at first, it was considered the size percentage obtained from the Laser Scattering analysis, for the specific range needed.

As known, for each sample it was used 514g of sand (stabilized by a prefixed proportionality ratio), which was screened and separated in other fractions: <200, 200, 315, 500, etc.

As it can be read in Table 2, for each series there is a percentage of fraction related to the amount of particle size with that specific range present in the sample created. So, to find the cumulative fraction that can be related then to the size percentage, it is useful to apply this simple formula:

$$\Sigma F(x) = \% \text{ sand fraction} * \text{distribution} + \% \text{ sand fraction} * \text{distribution}$$

Let's see clearly with an example: series A is made up with 50% sand <sub>500</sub> and 50% sand <sub>315</sub>. That means 257g is sand <sub>500</sub> and 257g is sand <sub>315</sub>.

In order to explain how the last column on the Table 2 is obtained, the following formula has to be applied:

$$\Sigma F(x) = (0,5 * F(x)_1) + (0,5 * F(x)_2) \quad (1)$$

Where,

- $F(x)_1$  is the % of sand distribution for the fraction 315;
- $F(x)_2$  is the % of sand distribution for the fraction 500.

Table 2- Series A: sand distribution analysis

Series A: 50% -50%			
size %	F(x)1 [315]	F(x)2 [500]	ΣF(x)
0,011	0	0	0
0,013	0	0	0
0,015	0	0	0
0,017	0	0	0
0,02	0	0	0
0,023	0	0	0
0,026	0	0	0
0,03	0	0	0
0,034	0	0	0
0,039	0	0	0
0,044	0	0	0
0,051	0	0	0
0,058	0	0	0
0,067	0	0	0
0,076	0	0	0
0,087	0	0	0
0,1	0	0	0
0,115	0	0	0
0,131	0	0	0
0,15	0	0	0
0,172	0	0	0
0,197	0	0	0
0,226	0	0	0

0,259	0	0	0
0,296	0	0	0
0,339	0	0	0
0,389	0	0	0
0,445	0	0	0
0,51	0	0	0
0,584	0	0	0
0,669	0	0	0
0,766	0	0	0
0,877	0	0	0
1,005	0	0	0
1,151	0	0	0
1,318	0	0	0
1,51	0	0	0
1,729	0	0	0
1,981	0	0	0
2,269	0	0	0
2,599	0	0	0
2,976	0	0	0
3,409	0	0	0
3,905	0	0	0
4,472	0	0	0
5,122	0	0	0
5,867	0	0	0
6,72	0	0	0
7,697	0	0	0
8,816	0	0	0
10,097	0	0	0
11,565	0	0	0
13,246	0	0	0
15,172	0	0	0
17,377	0	0	0
19,904	0	0	0
22,797	0	0	0
26,111	0	0	0
29,907	0	0	0
34,255	0	0	0
39,234	0	0	0
44,938	0	0	0
51,471	0	0	0
58,953	0	0,125	0,0625
67,523	0	0,289	0,1445
77,34	0	0,507	0,2535
88,583	0,135	0,811	0,4055
101,46	0,33	1,249	0,6245

116,21	0,626	1,89	0,945
133,103	1,16	2,919	1,4595
152,453	2,278	4,655	2,3275
174,616	4,833	7,579	3,7895
200	10,783	12,313	6,1565
229,075	23,207	19,442	9,721
262,376	42,971	29,206	14,603
300,518	64,616	41,31	20,655
344,206	81,224	54,843	27,4215
394,244	91,145	68,295	34,1475
451,556	96,23	79,8	39,9
517,2	98,562	88,181	44,0905
592,387	99,569	93,597	46,7985
678,504	100	96,791	48,3955
777,141	100	98,539	49,2695
890,116	100	99,478	49,739
1019,515	100	100	50
1167,725	100	100	50
1337,481	100	100	50
1531,914	100	100	50
1754,613	100	100	50
2009,687	100	100	50
2301,841	100	100	50
2636,467	100	100	50
3000	100	100	50

Table 3- Series B: sand distribution analysis

Series B: 70%- 30%			
size %	F(x)1 [315]	F(x)2 [500]	$\Sigma F(x)$
0,011	0	0	0
0,013	0	0	0
0,015	0	0	0
0,017	0	0	0
0,02	0	0	0
0,023	0	0	0
0,026	0	0	0
0,03	0	0	0
0,034	0	0	0
0,039	0	0	0
0,044	0	0	0
0,051	0	0	0
0,058	0	0	0
0,067	0	0	0
0,076	0	0	0
0,087	0	0	0

0,1	0	0	0
0,115	0	0	0
0,131	0	0	0
0,15	0	0	0
0,172	0	0	0
0,197	0	0	0
0,226	0	0	0
0,259	0	0	0
0,296	0	0	0
0,339	0	0	0
0,389	0	0	0
0,445	0	0	0
0,51	0	0	0
0,584	0	0	0
0,669	0	0	0
0,766	0	0	0
0,877	0	0	0
1,005	0	0	0
1,151	0	0	0
1,318	0	0	0
1,51	0	0	0
1,729	0	0	0
1,981	0	0	0
2,269	0	0	0
2,599	0	0	0
2,976	0	0	0
3,409	0	0	0
3,905	0	0	0
4,472	0	0	0
5,122	0	0	0
5,867	0	0	0
6,72	0	0	0
7,697	0	0	0
8,816	0	0	0
10,097	0	0	0
11,565	0	0	0
13,246	0	0	0
15,172	0	0	0
17,377	0	0	0
19,904	0	0	0
22,797	0	0	0
26,111	0	0	0
29,907	0	0	0
34,255	0	0	0
39,234	0	0	0

44,938	0	0	0
51,471	0	0	0
58,953	0	0,125	0,0375
67,523	0	0,289	0,0867
77,34	0	0,507	0,1521
88,583	0,135	0,811	0,3378
101,46	0,33	1,249	0,6057
116,21	0,626	1,89	1,0052
133,103	1,16	2,919	1,6877
152,453	2,278	4,655	2,9911
174,616	4,833	7,579	5,6568
200	10,783	12,313	11,242
229,075	23,207	19,442	22,0775
262,376	42,971	29,206	38,8415
300,518	64,616	41,31	57,6242
344,206	81,224	54,843	73,3097
394,244	91,145	68,295	84,29
451,556	96,23	79,8	91,301
517,2	98,562	88,181	95,4477
592,387	99,569	93,597	97,7774
678,504	100	96,791	99,0373
777,141	100	98,539	99,5617
890,116	100	99,478	99,8434
1019,515	100	100	100
1167,725	100	100	100
1337,481	100	100	100
1531,914	100	100	100
1754,613	100	100	100
2009,687	100	100	100
2301,841	100	100	100
2636,467	100	100	100
3000	100	100	100

Table 4- Series C: sand distribution analysis

Series C: 50%- 50%			
size %	F(x)1 [200]	F(x)2 [<200]	ΣF(x)
0,011	0	0	0
0,013	0	0	0
0,015	0	0	0
0,017	0	0	0
0,02	0	0	0
0,023	0	0	0
0,026	0	0	0
0,03	0	0	0
0,034	0	0	0

0,039	0	0	0
0,044	0	0	0
0,051	0	0	0
0,058	0	0	0
0,067	0	0	0
0,076	0	0	0
0,087	0	0	0
0,1	0	0	0
0,115	0	0	0
0,131	0	0	0
0,15	0	0	0
0,172	0	0	0
0,197	0	0	0
0,226	0	0	0
0,259	0	0	0
0,296	0	0	0
0,339	0	0	0
0,389	0	0	0
0,445	0	0	0
0,51	0	0	0
0,584	0	0	0
0,669	0	0	0
0,766	0	0	0
0,877	0	0	0
1,005	0	0	0
1,151	0	0	0
1,318	0	0	0
1,51	0	0	0
1,729	0	0,113	0,0565
1,981	0	0,238	0,119
2,269	0	0,369	0,1845
2,599	0	0,498	0,249
2,976	0	0,621	0,3105
3,409	0	0,733	0,3665
3,905	0	0,733	0,3665
4,472	0	0,733	0,3665
5,122	0	0,733	0,3665
5,867	0	0,733	0,3665
6,72	0	0,733	0,3665
7,697	0	0,733	0,3665
8,816	0	0,733	0,3665
10,097	0	0,733	0,3665
11,565	0	0,733	0,3665
13,246	0	0,733	0,3665
15,172	0	0,733	0,3665

17,377	0	0,733	0,3665
19,904	0	0,733	0,3665
22,797	0	0,733	0,3665
26,111	0	0,733	0,3665
29,907	0	0,733	0,3665
34,255	0	0,733	0,3665
39,234	0	0,733	0,3665
44,938	0	0,733	0,3665
51,471	0	0,733	0,3665
58,953	0	0,733	0,3665
67,523	0	0,733	0,3665
77,34	0	0,863	0,4315
88,583	0,135	1,153	0,644
101,46	0,33	1,877	1,1035
116,21	0,626	3,682	2,154
133,103	1,16	8,18	4,67
152,453	2,278	17,862	10,07
174,616	4,833	34,414	19,6235
200	10,783	55,335	33,059
229,075	23,207	74,169	48,688
262,376	42,971	86,768	64,8695
300,518	64,616	93,728	79,172
344,206	81,224	97,208	89,216
394,244	91,145	98,849	94,997
451,556	96,23	99,589	97,9095
517,2	98,562	100	99,281
592,387	99,569	100	99,7845
678,504	100	100	100
777,141	100	100	100
890,116	100	100	100
1019,515	100	100	100
1167,725	100	100	100
1337,481	100	100	100
1531,914	100	100	100
1754,613	100	100	100
2009,687	100	100	100
2301,841	100	100	100
2636,467	100	100	100
3000	100	100	100

Table 5- Series D: sand distribution analysis

Series D: 50%- 50%			
size %	F(x)1 [315]	F(x)2 [200]	$\Sigma F(x)$
0,011	0	0	0
0,013	0	0	0

0,015	0	0	0
0,017	0	0	0
0,02	0	0	0
0,023	0	0	0
0,026	0	0	0
0,03	0	0	0
0,034	0	0	0
0,039	0	0	0
0,044	0	0	0
0,051	0	0	0
0,058	0	0	0
0,067	0	0	0
0,076	0	0	0
0,087	0	0	0
0,1	0	0	0
0,115	0	0	0
0,131	0	0	0
0,15	0	0	0
0,172	0	0	0
0,197	0	0	0
0,226	0	0	0
0,259	0	0	0
0,296	0	0	0
0,339	0	0	0
0,389	0	0	0
0,445	0	0	0
0,51	0	0	0
0,584	0	0	0
0,669	0	0	0
0,766	0	0	0
0,877	0	0	0
1,005	0	0	0
1,151	0	0	0
1,318	0	0	0
1,51	0	0	0
1,729	0	0,113	0,0565
1,981	0	0,238	0,119
2,269	0	0,369	0,1845
2,599	0	0,498	0,249
2,976	0	0,621	0,3105
3,409	0	0,733	0,3665
3,905	0	0,733	0,3665
4,472	0	0,733	0,3665
5,122	0	0,733	0,3665
5,867	0	0,733	0,3665

6,72	0	0,733	0,3665
7,697	0	0,733	0,3665
8,816	0	0,733	0,3665
10,097	0	0,733	0,3665
11,565	0	0,733	0,3665
13,246	0	0,733	0,3665
15,172	0	0,733	0,3665
17,377	0	0,733	0,3665
19,904	0	0,733	0,3665
22,797	0	0,733	0,3665
26,111	0	0,733	0,3665
29,907	0	0,733	0,3665
34,255	0	0,733	0,3665
39,234	0	0,733	0,3665
44,938	0	0,733	0,3665
51,471	0	0,733	0,3665
58,953	0	0,733	0,3665
67,523	0	0,733	0,3665
77,34	0	0,863	0,4315
88,583	0,135	1,153	0,644
101,46	0,33	1,877	1,1035
116,21	0,626	3,682	2,154
133,103	1,16	8,18	4,67
152,453	2,278	17,862	10,07
174,616	4,833	34,414	19,6235
200	10,783	55,335	33,059
229,075	23,207	74,169	48,688
262,376	42,971	86,768	64,8695
300,518	64,616	93,728	79,172
344,206	81,224	97,208	89,216
394,244	91,145	98,849	94,997
451,556	96,23	99,589	97,9095
517,2	98,562	100	99,281
592,387	99,569	100	99,7845
678,504	100	100	100
777,141	100	100	100
890,116	100	100	100
1019,515	100	100	100
1167,725	100	100	100
1337,481	100	100	100
1531,914	100	100	100
1754,613	100	100	100
2009,687	100	100	100
2301,841	100	100	100
2636,467	100	100	100

3000	100	100	100
------	-----	-----	-----

Table 6- Series E: sand distribution analysis

Series E: 50%- 50%			
size %	F(x)1 [315]	F(x)2 [<200]	ΣF(x)
0,011	0	0	0
0,013	0	0	0
0,015	0	0	0
0,017	0	0	0
0,02	0	0	0
0,023	0	0	0
0,026	0	0	0
0,03	0	0	0
0,034	0	0	0
0,039	0	0	0
0,044	0	0	0
0,051	0	0	0
0,058	0	0	0
0,067	0	0	0
0,076	0	0	0
0,087	0	0	0
0,1	0	0	0
0,115	0	0	0
0,131	0	0	0
0,15	0	0	0
0,172	0	0	0
0,197	0	0	0
0,226	0	0	0
0,259	0	0	0
0,296	0	0	0
0,339	0	0,134	0,067
0,389	0	0,335	0,1675
0,445	0	0,605	0,3025
0,51	0	0,927	0,4635
0,584	0	1,267	0,6335
0,669	0	1,585	0,7925
0,766	0	1,852	0,926
0,877	0	2,052	1,026
1,005	0	2,19	1,095
1,151	0	2,19	1,095
1,318	0	2,19	1,095
1,51	0	2,19	1,095
1,729	0	2,19	1,095
1,981	0	2,19	1,095
2,269	0	2,19	1,095

2,599	0	2,19	1,095
2,976	0	2,19	1,095
3,409	0	2,297	1,1485
3,905	0	2,426	1,213
4,472	0	2,582	1,291
5,122	0	2,77	1,385
5,867	0	2,995	1,4975
6,72	0	3,266	1,633
7,697	0	3,591	1,7955
8,816	0	3,984	1,992
10,097	0	4,453	2,2265
11,565	0	4,999	2,4995
13,246	0	5,645	2,8225
15,172	0	6,426	3,213
17,377	0	7,382	3,691
19,904	0	8,545	4,2725
22,797	0	9,934	4,967
26,111	0	11,557	5,7785
29,907	0	13,425	6,7125
34,255	0	15,573	7,7865
39,234	0	18,105	9,0525
44,938	0	21,209	10,6045
51,471	0	25,066	12,533
58,953	0	29,882	14,941
67,523	0	35,913	17,9565
77,34	0	43,334	21,667
88,583	0,135	52,383	26,259
101,46	0,33	63,525	31,9275
116,21	0,626	76,162	38,394
133,103	1,16	85,683	43,4215
152,453	2,278	91,698	46,988
174,616	4,833	95,374	50,1035
200	10,783	97,569	54,176
229,075	23,207	98,853	61,03
262,376	42,971	99,59	71,2805
300,518	64,616	100	82,308
344,206	81,224	100	90,612
394,244	91,145	100	95,5725
451,556	96,23	100	98,115
517,2	98,562	100	99,281
592,387	99,569	100	99,7845
678,504	100	100	100
777,141	100	100	100
890,116	100	100	100
1019,515	100	100	100

1167,725	100	100	100
1337,481	100	100	100
1531,914	100	100	100
1754,613	100	100	100
2009,687	100	100	100
2301,841	100	100	100
2636,467	100	100	100
3000	100	100	100

Table 7- Series F: sand distribution analysis

Series F: 70%-30%			
size %	F(x)1 [500]	F(x)2 [315]	$\Sigma F(x)$
0,011	0	0	0
0,013	0	0	0
0,015	0	0	0
0,017	0	0	0
0,02	0	0	0
0,023	0	0	0
0,026	0	0	0
0,03	0	0	0
0,034	0	0	0
0,039	0	0	0
0,044	0	0	0
0,051	0	0	0
0,058	0	0	0
0,067	0	0	0
0,076	0	0	0
0,087	0	0	0
0,1	0	0	0
0,115	0	0	0
0,131	0	0	0
0,15	0	0	0
0,172	0	0	0
0,197	0	0	0
0,226	0	0	0
0,259	0	0	0
0,296	0	0	0
0,339	0	0	0
0,389	0	0	0
0,445	0	0	0
0,51	0	0	0
0,584	0	0	0
0,669	0	0	0
0,766	0	0	0
0,877	0	0	0

1,005	0	0	0
1,151	0	0	0
1,318	0	0	0
1,51	0	0	0
1,729	0	0	0
1,981	0	0	0
2,269	0	0	0
2,599	0	0	0
2,976	0	0	0
3,409	0	0	0
3,905	0	0	0
4,472	0	0	0
5,122	0	0	0
5,867	0	0	0
6,72	0	0	0
7,697	0	0	0
8,816	0	0	0
10,097	0	0	0
11,565	0	0	0
13,246	0	0	0
15,172	0	0	0
17,377	0	0	0
19,904	0	0	0
22,797	0	0	0
26,111	0	0	0
29,907	0	0	0
34,255	0	0	0
39,234	0	0	0
44,938	0	0	0
51,471	0	0	0
58,953	0,125	0	0,0875
67,523	0,289	0	0,2023
77,34	0,507	0	0,3549
88,583	0,811	0,135	0,6082
101,46	1,249	0,33	0,9733
116,21	1,89	0,626	1,5108
133,103	2,919	1,16	2,3913
152,453	4,655	2,278	3,9419
174,616	7,579	4,833	6,7552
200	12,313	10,783	11,854
229,075	19,442	23,207	20,5715
262,376	29,206	42,971	33,3355
300,518	41,31	64,616	48,3018
344,206	54,843	81,224	62,7573
394,244	68,295	91,145	75,15

451,556	79,8	96,23	84,729
517,2	88,181	98,562	91,2953
592,387	93,597	99,569	95,3886
678,504	96,791	100	97,7537
777,141	98,539	100	98,9773
890,116	99,478	100	99,6346
1019,515	100	100	100
1167,725	100	100	100
1337,481	100	100	100
1531,914	100	100	100
1754,613	100	100	100
2009,687	100	100	100
2301,841	100	100	100
2636,467	100	100	100
3000	100	100	100

Table 8- Series G: sand distribution analysis

Series G: 25%-25%-25%-25%					
size %	F(x)1 [<200]	F(x)2 [200]	F(x)3 [315]	F(x)4 [500]	ΣF(x)
0,011	0	0	0	0	0
0,013	0	0	0	0	0
0,015	0	0	0	0	0
0,017	0	0	0	0	0
0,02	0	0	0	0	0
0,023	0	0	0	0	0
0,026	0	0	0	0	0
0,03	0	0	0	0	0
0,034	0	0	0	0	0
0,039	0	0	0	0	0
0,044	0	0	0	0	0
0,051	0	0	0	0	0
0,058	0	0	0	0	0
0,067	0	0	0	0	0
0,076	0	0	0	0	0
0,087	0	0	0	0	0
0,1	0	0	0	0	0
0,115	0	0	0	0	0
0,131	0	0	0	0	0
0,15	0	0	0	0	0
0,172	0	0	0	0	0
0,197	0	0	0	0	0
0,226	0	0	0	0	0
0,259	0	0	0	0	0
0,296	0	0	0	0	0
0,339	0,134	0	0	0	0,0335

0,389	0,335	0	0	0	0,08375
0,445	0,605	0	0	0	0,15125
0,51	0,927	0	0	0	0,23175
0,584	1,267	0	0	0	0,31675
0,669	1,585	0	0	0	0,39625
0,766	1,852	0	0	0	0,463
0,877	2,052	0	0	0	0,513
1,005	2,19	0	0	0	0,5475
1,151	2,19	0	0	0	0,5475
1,318	2,19	0	0	0	0,5475
1,51	2,19	0	0	0	0,5475
1,729	2,19	0,113	0	0	0,57575
1,981	2,19	0,238	0	0	0,607
2,269	2,19	0,369	0	0	0,63975
2,599	2,19	0,498	0	0	0,672
2,976	2,19	0,621	0	0	0,70275
3,409	2,297	0,733	0	0	0,7575
3,905	2,426	0,733	0	0	0,78975
4,472	2,582	0,733	0	0	0,82875
5,122	2,77	0,733	0	0	0,87575
5,867	2,995	0,733	0	0	0,932
6,72	3,266	0,733	0	0	0,99975
7,697	3,591	0,733	0	0	1,081
8,816	3,984	0,733	0	0	1,17925
10,097	4,453	0,733	0	0	1,2965
11,565	4,999	0,733	0	0	1,433
13,246	5,645	0,733	0	0	1,5945
15,172	6,426	0,733	0	0	1,78975
17,377	7,382	0,733	0	0	2,02875
19,904	8,545	0,733	0	0	2,3195
22,797	9,934	0,733	0	0	2,66675
26,111	11,557	0,733	0	0	3,0725
29,907	13,425	0,733	0	0	3,5395
34,255	15,573	0,733	0	0	4,0765
39,234	18,105	0,733	0	0	4,7095
44,938	21,209	0,733	0	0	5,4855
51,471	25,066	0,733	0	0	6,44975
58,953	29,882	0,733	0	0,125	7,685
67,523	35,913	0,733	0	0,289	9,23375
77,34	43,334	0,863	0	0,507	11,176
88,583	52,383	1,153	0,135	0,811	13,6205
101,46	63,525	1,877	0,33	1,249	16,74525
116,21	76,162	3,682	0,626	1,89	20,59
133,103	85,683	8,18	1,16	2,919	24,4855
152,453	91,698	17,862	2,278	4,655	29,12325

174,616	95,374	34,414	4,833	7,579	35,55
200	97,569	55,335	10,783	12,313	44
229,075	98,853	74,169	23,207	19,442	53,91775
262,376	99,59	86,768	42,971	29,206	64,63375
300,518	100	93,728	64,616	41,31	74,9135
344,206	100	97,208	81,224	54,843	83,31875
394,244	100	98,849	91,145	68,295	89,57225
451,556	100	99,589	96,23	79,8	93,90475
517,2	100	100	98,562	88,181	96,68575
592,387	100	100	99,569	93,597	98,2915
678,504	100	100	100	96,791	99,19775
777,141	100	100	100	98,539	99,63475
890,116	100	100	100	99,478	99,8695
1019,515	100	100	100	100	100
1167,725	100	100	100	100	100
1337,481	100	100	100	100	100
1531,914	100	100	100	100	100
1754,613	100	100	100	100	100
2009,687	100	100	100	100	100
2301,841	100	100	100	100	100
2636,467	100	100	100	100	100
3000	100	100	100	100	100

Table 9- Series H: sand distribution analysis

Series H: 35%-65%			
size %	F(x)1 [315]	F(x)2 [500]	$\Sigma F(x)$
0,011	0	0	0
0,013	0	0	0
0,015	0	0	0
0,017	0	0	0
0,02	0	0	0
0,023	0	0	0
0,026	0	0	0
0,03	0	0	0
0,034	0	0	0
0,039	0	0	0
0,044	0	0	0
0,051	0	0	0
0,058	0	0	0
0,067	0	0	0
0,076	0	0	0
0,087	0	0	0
0,1	0	0	0
0,115	0	0	0
0,131	0	0	0

0,15	0	0	0
0,172	0	0	0
0,197	0	0	0
0,226	0	0	0
0,259	0	0	0
0,296	0	0	0
0,339	0	0	0
0,389	0	0	0
0,445	0	0	0
0,51	0	0	0
0,584	0	0	0
0,669	0	0	0
0,766	0	0	0
0,877	0	0	0
1,005	0	0	0
1,151	0	0	0
1,318	0	0	0
1,51	0	0	0
1,729	0	0	0
1,981	0	0	0
2,269	0	0	0
2,599	0	0	0
2,976	0	0	0
3,409	0	0	0
3,905	0	0	0
4,472	0	0	0
5,122	0	0	0
5,867	0	0	0
6,72	0	0	0
7,697	0	0	0
8,816	0	0	0
10,097	0	0	0
11,565	0	0	0
13,246	0	0	0
15,172	0	0	0
17,377	0	0	0
19,904	0	0	0
22,797	0	0	0
26,111	0	0	0
29,907	0	0	0
34,255	0	0	0
39,234	0	0	0
44,938	0	0	0
51,471	0	0	0
58,953	0	0,125	0,08125

67,523	0	0,289	0,18785
77,34	0	0,507	0,32955
88,583	0,135	0,811	0,5744
101,46	0,33	1,249	0,92735
116,21	0,626	1,89	1,4476
133,103	1,16	2,919	2,30335
152,453	2,278	4,655	3,82305
174,616	4,833	7,579	6,6179
200	10,783	12,313	11,7775
229,075	23,207	19,442	20,75975
262,376	42,971	29,206	34,02375
300,518	64,616	41,31	49,4671
344,206	81,224	54,843	64,07635
394,244	91,145	68,295	76,2925
451,556	96,23	79,8	85,5505
517,2	98,562	88,181	91,81435
592,387	99,569	93,597	95,6872
678,504	100	96,791	97,91415
777,141	100	98,539	99,05035
890,116	100	99,478	99,6607
1019,515	100	100	100
1167,725	100	100	100
1337,481	100	100	100
1531,914	100	100	100
1754,613	100	100	100
2009,687	100	100	100
2301,841	100	100	100
2636,467	100	100	100
3000	100	100	100

The value of  $\Sigma F(x)$  can be represented graphically to see how the distribution for each series of created samples looks like. Therefore, to have a perfect graph, here it was used the software Grapher 6, which helped to get the following representations. For each series, it is possible to observe a graph, on which the x-axis is the % size and the y-axis is the cumulative calculated fraction,  $F(x)$ .

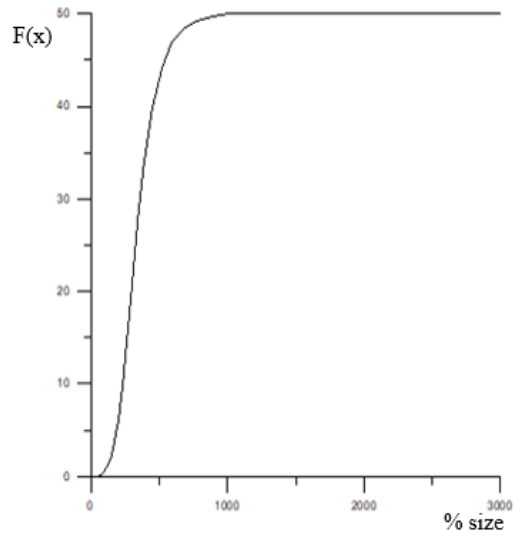


Figure 2- Series A

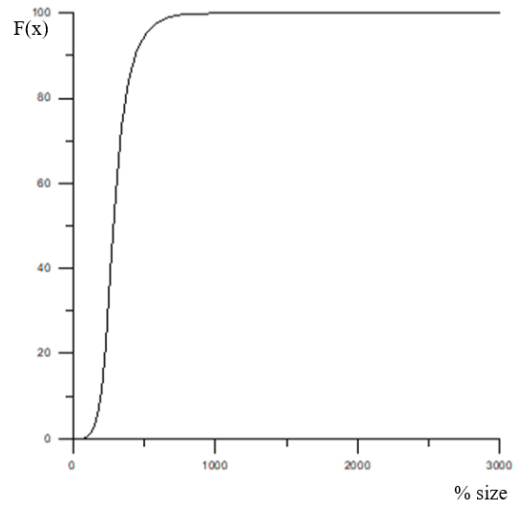


Figure 3- Series B

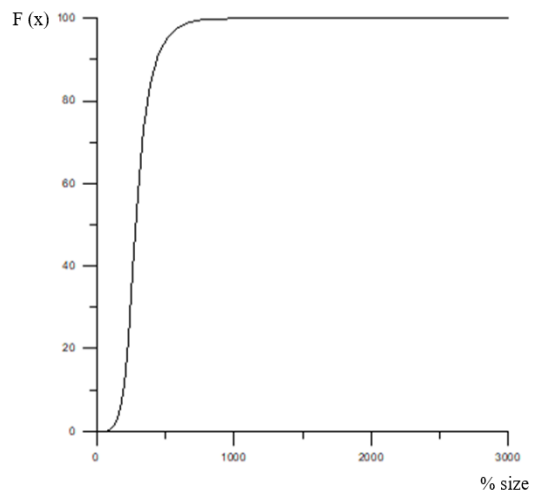


Figure 4- Series C

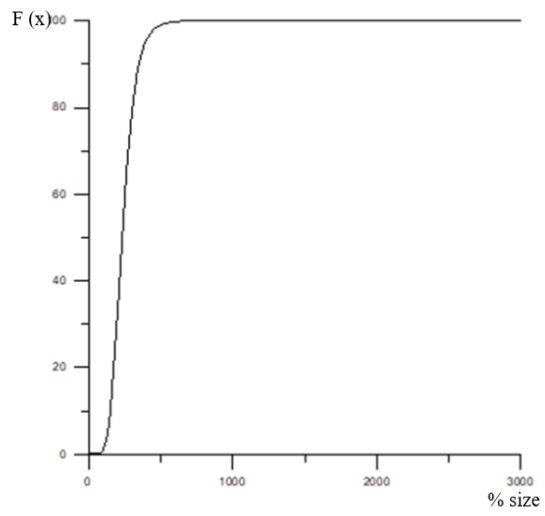


Figure 5- Series D

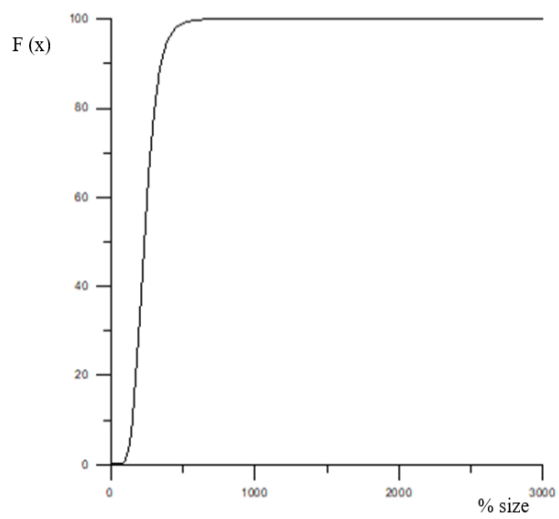


Figure 6- Series E

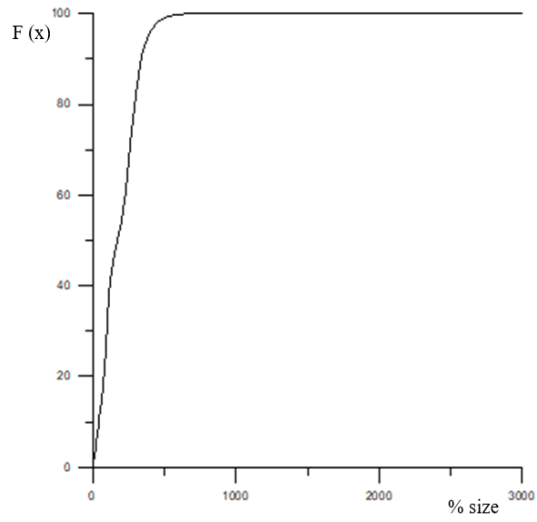


Figure 7- Series F

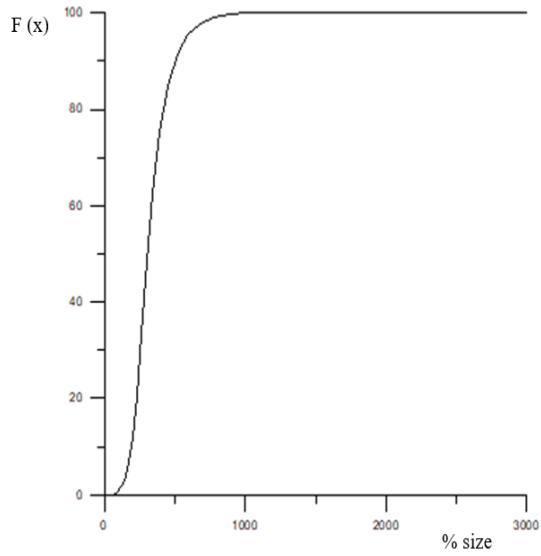


Figure 8- Series G

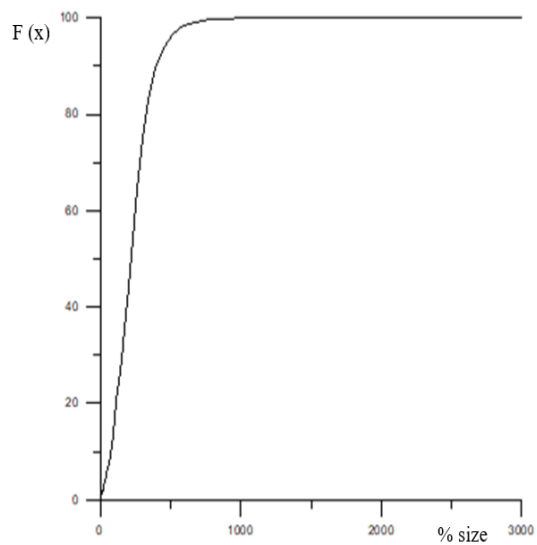


Figure 9- Series H

The trends obtained shown a different curve each because characterized by a grain size distribution which differs series by series.

Every curve can be described by a mathematical function expressed by an equation. In particular, for this case three are the types you can use:

1. **Schumman- Gaudin** :  $y = POW (x / a,m )$ ;
2. **Rosin – Rammler (50% - Oshoz)** :  $y = 1 - \exp ( \ln( 2* POW (x / a,m )$ );
3. **Rosin – Rammler (63,2 % - Oshoz)** :  $y = 1 - \exp ( \ln ( 2* POW( x/ a,m)$ .

The best one which fits more perfectly for the description of the curve trend in this case is the first equation, the Shumman – Gaudin.

From the mentioned equation you get “m” value, which corresponds on the slope of the curve and you have a characteristic properties of the series. This value can be put in relation with the other properties, such as porosity and permeability, to show the influence of particle size distribution on them.

For lack of time, it was not possible to show mathematically that; therefore, it was used the mean radius of the particle size of each series with the properties analyzed in this work.

You will see better in chapt 4th.

### THIRD CHAPTER

#### **“LAB ANALYSES ON THE CREATED SAND SPECIMENS”**

##### *3.1 “Helium Porosimeter”*

The Helium Porosimeter is the instrument that permits to determine the grain and pore volume of samples by means of the gas expansion governed by Boyle- Mariott’s law,  $P_1 V_1 = P_2 V_2$ , from which derives the value of porosity.

By recalling some theoretical concept, porosity is found as the ratio of the pore volume to the bulk volume of a porous medium:

$$\emptyset = \frac{V_p}{V_t} = \frac{V_t - V_s}{V_t} \quad (2)$$

Where,

- $V_p$  is the pore volume, [m<sup>3</sup>];
- $V_t$  is the total volume (bulk volume), [m<sup>3</sup>];
- $V_s$  is the solid volume, [m<sup>3</sup>].

Helium source is a Helium tank connected to a porosimeter: so, at first you need to open the valve that keeps the gas inside. Helium isothermally expands into a chamber of known volume and pressure till the equilibrium is reached.

Then, you can put your core into a specific chamber of volume  $V_1$  and pressure  $P_1$ , seal off in order to not have any leakages.

As a second step you can turn on the two valves, allowing the expansion of the gas and very quickly turn off again. It is possible to read the initial pressure value,  $P_0$ , on the manometer. Then, by switching off the valves of the gas, you can read the second value of pressure,  $P_2$  of the relative core after gas has expanded.

Input parameters are: sample diameter, length, weight and the pressure given by the device. So, basically you are able to measure the bulk volume.

$$p_1(V_1 - V_s) + p_0V_2 = p_2(V_1 + V_2 - V_s) \quad (3)$$

Where:

- $P_0$  is the initial pressure value that you can read on the manometer;
- $P_1$  is the value of pressure of the sample when put firstly in the chamber;
- $P_2$  is the final pressure after gas expansion;
- $V_1$  is the volume of the core when firstly put in the chamber;
- $V_2$  the final volume;

- $V_s$  is the volume of the solid.

Since the size of the samples is non precise, you will take three different values on the top, in the middle, and on the bottom of the specimen, for length parameters.

The reasons why Helium is used to perform this kind of analysis are several and consistent: it is a gas that has low mass and high diffusivity, particularly important those for low permeability rocks; it is formed by small molecules which will penetrate the tiny pores; and then, it can be considered as an ideal gas for most pressure and temperature measurements, (Faisal Muhammad, *Helium Porosimeter*).

The first approach in porosity measurements was driven by this way, using the above described method. But the device had some problem and was not working during the time of examination, so another method has been adopted, efficient as well. Let's see the procedure in the next paragraph.

### 3.2 Porosity measurements

In order to get the porosity, it was adopted an empirical method according to which it is possible to find  $\phi$  through VBA editor, a coding program that works with excel.

At first, for each sample you need to measure 3 times diameter (upper, middle and down part) and length by an electronic device, a caliper. Then, you can measure dry mass by a precise scale.

After this step, you water the cores for 1 day by using distillate water and when you took them off, you did vacuum at very low pressure, typically  $0,1 \text{ kg/cm}^2$ . This because you do not want to reach the boiling point (in fact, at low pressure, boiling temperature decreases).

After that, it is possible to get the wetting mass, used together with all the other information to find porosity. Then, through the Visual Basic for Application it easy to get the values of permeability by means of simple formula that put together the parameters showed in the following, Tab 10.

Table 10- Porosity measurements

Sample	d <sub>1</sub> [cm]	d <sub>2</sub> [cm]	d <sub>3</sub> [cm]	L <sub>1</sub> [cm]	L <sub>2</sub> [cm]	L <sub>3</sub> [cm]	m <sub>dry</sub> [g]	m <sub>wet</sub> [g]	$\Phi$ [-]
A1	3,805	3,2	3,6	6,2	6	5,8	80	96	0,271706
A2	3,785	3,218	3,799	5,128	5,153	5,119	97,716	116,48	0,35898
A3	3,798	3,792	3,786	5,175	5,148	5,196	96,352	115,71	0,331353
1B	3,818	3,829	3,792	5,0321	5,061	5,036	92,384	109,92	0,30452
2C	3,737	3,777	3,756	5	4,93	4,999	94,626	112,98	0,332756
2D	3,916	3,938	3,888	4,647	4,646	4,624	91,895	109,61	0,317384
3D	3,945	3,944	3,957	4,462	4,538	4,58	93,077	110,29	0,310518
1E	3,926	3,97	3,936	4,588	4,584	4,585	98	115,61	0,317298
2E	3,927	3,985	3,999	4,559	4,544	4,494	97,801	115,103	0,308341
3E	3,942	3,962	3,941	4,513	4,427	4,38	90,74	107,08	0,300574
F1	3,958	3,968	3,94	4,609	4,686	4,711	92,545	109,7	0,299049
F2	3,881	3,923	3,901	4,605	4,632	4,683	94,877	112,1	0,310456
G1	3,779	3,815	3,802	5,045	4,993	4,993	95,614	113,57	0,316221
G2	3,811	3,804	3,794	4,681	4,736	4,802	92,384	109,51	0,318101
G3	3,77	3,774	3,762	4,426	4,448	4,374	84,002	100,34	0,331669
H2	3,78	3,744	3,726	5,243	5,237	5,186	98,939	115,96	0,295118
H4	3,739	3,741	3,777	5,15	5,212	5,241	96,451	114,12	0,307208

The obtained values of porosity change slightly for each series, but it is a little difference since the main fractions used are almost the same in a different percentage.

For sure, it can be said that a relation exists between porosity and particle size distribution, but it will be discussed later, in chapter 4<sup>th</sup>.

### 3.3 Permeability measurements

The value of permeability can be derived from the Darcy's equation, that describes the linear relationship between the flow rate through a porous medium of permeability  $k$ , the viscosity of the fluid  $\mu$ , and the pressure drop  $\Delta P$ , for a homogeneous porous medium and in absence of gravitational forces:

$$k = \frac{q \mu L}{A \Delta P} \quad (4)$$

In order to measure permeability of each core the gas permeameter was used: the specimen was put into the holder, covered up by a rubber container which allows to get the core permeability only and does not permit the flow to enter in between core and rubber.

To get the outside pressure it was used distillate water; while for the inlet pressure you need to measure it; then nitrogen is used for gas flowing and from this the dynamic viscosity was retrieved. The reason why you use nitrogen is due to its availability, cost and minimization of fluid-rock reaction.

You need to consider the flow rate region where the pressure remains proportional to flow rate within the experimental error.

So, the device works with a rotometer that measures the gas flow rate. In fact, once the gas is flown, the ball rises up and you can read the value directly from the tool. At low pressure it is assumed gas follows the ideal gas law (useful condition to apply the Darcy's law).

Once you get  $\mu$ , and you calculate the cross sectional area, the length, and the inlet pressure, you have all the necessary info to obtain the permeability.

The obtained values of permeability are shown below. As it is possible to observe the pressure levels for the imposed flow rates is considered as voltage, due to the fact that the gas permeameter gives these data information. Those values will be used into the VBA program, that will help with calculations for obtaining permeability.

Table 11- Permeability calculations for sample 2A

Sample		2A	
		pI (mbar)	1007
q (l/h)	$\Delta p$ (V)	TI (°C)	24
0	1,012	l (mm)	51,3
20	1,074	d (mm)	37,6
30	1,11		
40	1,147		
50	1,185		
60	1,226		
70	1,265		
80	1,31		
90	1,353		
100	1,395		

Table 12- Permeability calculations for sample 3A

Sample		3A	
		pI (mbar)	1007
q (l/h)	$\Delta p$ (V)	TI (°C)	24
0	1,012	l (mm)	44,3
20	1,18	d (mm)	38,2
30	1,265		
40	1,348		
50	1,433		
60	1,511		
70	1,59		
80	1,663		
90	1,742		
100	1,81		

Table 13- Permeability calculations for sample 1B

Sample		1B	
		pI (mbar)	1007
q (l/h)	$\Delta p$ (V)	TI (°C)	24
0	1,012	l (mm)	50,4
20	1,037	d (mm)	37,7
30	1,052		
40	1,065		
50	1,083		
60	1,101		
70	1,117		
80	1,133		
90	1,15		
100	1,17		

Table 14- Permeability calculations for sample 2C

Sample		2C	
		pI (mbar)	1007
q (l/h)	$\Delta p$ (V)	TI (°C)	24
0	1,012	l (mm)	50,1
20	1,153	d (mm)	37,7
30	1,225		
40	1,291		
50	1,355		
60	1,419		
70	1,481		
80	1,541		
90	1,603		
100	1,662		

Table 15- Permeability calculations for sample 2D

Sample		2D	
		pI (mbar)	1007
q (l/h)	$\Delta p$ (V)	TI (°C)	24
0	1,012	l (mm)	46,5
20	1,067	d (mm)	39,4
30	1,104		
40	1,136		
50	1,167		
60	1,2		
70	1,235		
80	1,267		
90	1,301		
100	1,337		

Table 16- Permeability calculations for sample 3D

Sample		3D	
		pI (mbar)	1,009
q (l/h)	$\Delta p$ (V)	TI (°C)	24
0	1,012	l (mm)	45,4
20	1,081	d (mm)	39,3
30	1,118		
40	1,159		
50	1,195		
60	1,242		
70	1,287		
80	1,335		
90	1,381		
100	1,424		

Table 17- Permeability calculations for sample 1E

Sample		1E	
		pl (mbar)	1007
q (l/h)	$\Delta p$ (V)	TI (°C)	24
0	1,012	l (mm)	45,8
20	1,257	d (mm)	39,6
30	1,386		
40	1,505		
50	1,62		
60	1,735		
70	1,838		
80	1,942		
90	2,048		
100	2,152		

Table 18- Permeability calculations for sample 2E

Sample		2E	
		pl (mbar)	1007
q (l/h)	$\Delta p$ (V)	TI (°C)	24
0	1,012	l (mm)	45,32
20	1,195	d (mm)	39,4
30	1,288		
40	1,372		
50	1,453		
60	1,542		
70	1,62		
80	1,702		
90	1,807		
100	1,889		

Table 19- Permeability calculations for sample 3E

Sample		3E	
		pl (mbar)	1,01
q (l/h)	$\Delta p$ (V)	TI (°C)	24
0	1,012	l (mm)	44,5
20	1,162	d (mm)	39,5
30	1,235		
40	1,304		
50	1,368		
60	1,437		
70	1,498		
80	1,556		
90	1,621		
100	1,678		

Table 20- Permeability calculations for sample 4E

Sample		4E	
		pl (mbar)	1,01
q (l/h)	$\Delta p$ (V)	TI (°C)	24
0	1,012	l (mm)	45,52
20	1,275	d (mm)	39,37
30	1,436		
40	1,58		
50	1,703		
60	1,826		
70	1,943		
80	2,004		
90	2,113		
100	2,22		

Table 21- Permeability calculations for sample F1

Sample		F1	
		pl (mbar)	1007
q (l/h)	$\Delta p$ (V)	TI (°C)	24
0	1,012	l (mm)	47
20	1,04	d (mm)	39,1
30	1,056		
40	1,072		
50	1,089		
60	1,108		
70	1,126		
80	1,146		
90	1,166		
100	1,187		

Table 22- Permeability calculations for sample F2

Sample		F2	
		pl (mbar)	1007
q (l/h)	$\Delta p$ (V)	TI (°C)	24
0	1,012	l (mm)	46,3
20	1,05	d (mm)	38,1
30	1,071		
40	1,093		
50	1,115		
60	1,139		
70	1,161		
80	1,187		
90	1,211		
100	1,237		

Table 23- Permeability calculations for sample G1

Sample		G1	
		pl (mbar)	1007
q (l/h)	$\Delta p$ (V)	TI (°C)	24
0	1,012	l (mm)	49,7
20	1,445	d (mm)	38,1
30	1,625		
40	1,772		
50	1,92		
60	2,06		
70	2,19		
80	2,305		
90	2,433		
100	2,552		

Table 24- Permeability calculations for sample G2

Sample		G2	
		pl (mbar)	1007
q (l/h)	$\Delta p$ (V)	TI (°C)	24
0	1,012	l (mm)	48
20	1,077	d (mm)	37,6
30	1,0121		
40	1,167		
50	1,218		
60	1,279		
70	1,344		
80	1,4		
90	1,469		
100	1,528		

Table 25- Permeability calculations for sample G3

Sample		G3	
		pl (mbar)	1,01
q (l/h)	$\Delta p$ (V)	TI (°C)	24
0	1,012	l (mm)	51,2
20	1,202	d (mm)	38,3
30	1,321		
40	1,424		
50	1,509		
60	1,608		
70	1,699		
80	1,795		
90	1,893		
100	1,988		

Table 26- Permeability calculations for sample H2

Sample		H2	
		pl (mbar)	1,009
q (l/h)	$\Delta p$ (V)	TI (°C)	24
0	1,012	l (mm)	52
20	1,046	d (mm)	37,7
30	1,066		
40	1,085		
50	1,104		
60	1,13		
70	1,152		
80	1,175		
90	1,199		
100	1,222		

Table 27- Permeability calculations for sample H3

Sample		H3	
		pl (mbar)	1,01
q (l/h)	$\Delta p$ (V)	TI (°C)	24
0	1,012	l (mm)	51,1
20	1,05	d (mm)	38,2
30	1,068		
40	1,09		
50	1,113		
60	1,138		
70	1,163		
80	1,184		
90	1,214		
100	1,239		

Table 28- Permeability calculations for sample H4

Sample		H4	
		pl (mbar)	1007
q (l/h)	$\Delta p$ (V)	TI (°C)	24
0	1,011	l (mm)	5
20	1,058	d (mm)	38,05
30	1,083		
40	1,108		
50	1,135		
60	1,163		
70	1,189		
80	1,218		
90	1,245		
100	1,274		

Besides, it is possible to see in the Table 29 the data referred to the laboratory properties and in Table 30 all the passages through which it is gotten the value of permeability, obtained in an immediate way with Visual Basic for Application with excel.

An example is reported by taking into account the core H4.

Table 29- Data

Lab. Properties	
Ta [°C]	24,0
Pa [bar]	1,0070
Gage type [bar]	6,89
Bar to atm conv.	0,9869
Rotameter const.	1,5
cm3/s to l/h	3,6
μN2 [cP]	0,017584
Voltage starts at [V]	1,013

$$k_g = k_{\infty} * \left[ 1 + \frac{b}{p_{avg}} \right]$$

$$q_a = - \frac{k_a * A}{\mu * L * P_a} * \left[ \frac{P_a^2 - P_1^2}{2} \right]$$

$$k_a = \frac{\mu * L * P_a}{A * \frac{1}{2} * B} \quad B = \left[ \frac{P_1^2 - P_a^2}{q_a} \right]$$

Table 30- Calculations for the value of Permeability

								Re-Calculated	
Qg	qg	Voltage P1	P1	P1 <sup>2</sup> -Pa <sup>2</sup>	1/Pavg	kg	(P1 <sup>2</sup> -Pa <sup>2</sup> )/qg	kg	(P1 <sup>2</sup> -Pa <sup>2</sup> )/qg
[l/hour]	[cm <sup>3</sup> /s]	[V]	[atm]	[atm <sup>2</sup> ]	[1/atm]	mD	[atm <sup>2</sup> /cm <sup>3</sup> /s]	mD	[atm <sup>2</sup> /cm <sup>3</sup> /s]
20	8,3333	1,058	1,0703	0,1579	0,96894	811,0652	0,01895	769,5756	0,0196
30	12,5000	1,083	1,1128	0,2507	0,94939	766,3207	0,02005	745,8151	0,0204
40	16,6667	1,108	1,1553	0,3471	0,93062	737,9885	0,02082	722,9942	0,0212
50	20,8333	1,135	1,2012	0,4552	0,91116	703,3085	0,02185	699,3403	0,0219
60	25,0000	1,163	1,2488	0,5718	0,89182	671,8600	0,02287	675,8329	0,0227
70	29,1667	1,189	1,2930	0,6842	0,87458	655,1309	0,02346	654,8809	0,0235
80	33,3333	1,218	1,3423	0,8141	0,85613	629,2395	0,02442	632,4466	0,0243
90	37,5000	1,245	1,3882	0,9394	0,83963	613,4574	0,02505	612,3943	0,0251
100	41,6667	1,274	1,4375	1,0787	0,82261	593,5987	0,02589	591,6999	0,0259

Table 31- Linear Regression 1 and Linear Regression 2

Linear regression 1 (k∞)		Linear regression 2 (kabs)		kg [mD]	-408
Slope	Intersection	Slope	Intersection	ka [mD]	854
1215,549546	-408,2175695	0,0002	0,0180		
46,21812424	40,04854923				
0,994250434	3,413737188				
691,7046565	4				
8060,850486	46,61440636				
"b" param.:	-2,9777				

What you obtain is a value of measured permeability to gas by considering the linear regression because as it was said before,  $k_g$  can be calculated as it would be a linear function of the type:

$$f(x) = A + B(x) \quad (5)$$

Where, A is the intercept, B the slope and “x” the function I want to investigate.

In this case,  $A = k_L$ .

To see the efficiency of the fitting you can use a coefficient of determination,  $R^2$  which can vary between 0-1. The closer is to the unity, the better is the fitting. An example is given right here, where by plotting values of the gas permeability into the y-axis and the fraction  $1/p_{avg}$  values, which is obtained by considering the average pressure values, into x-axis the following trend will be:

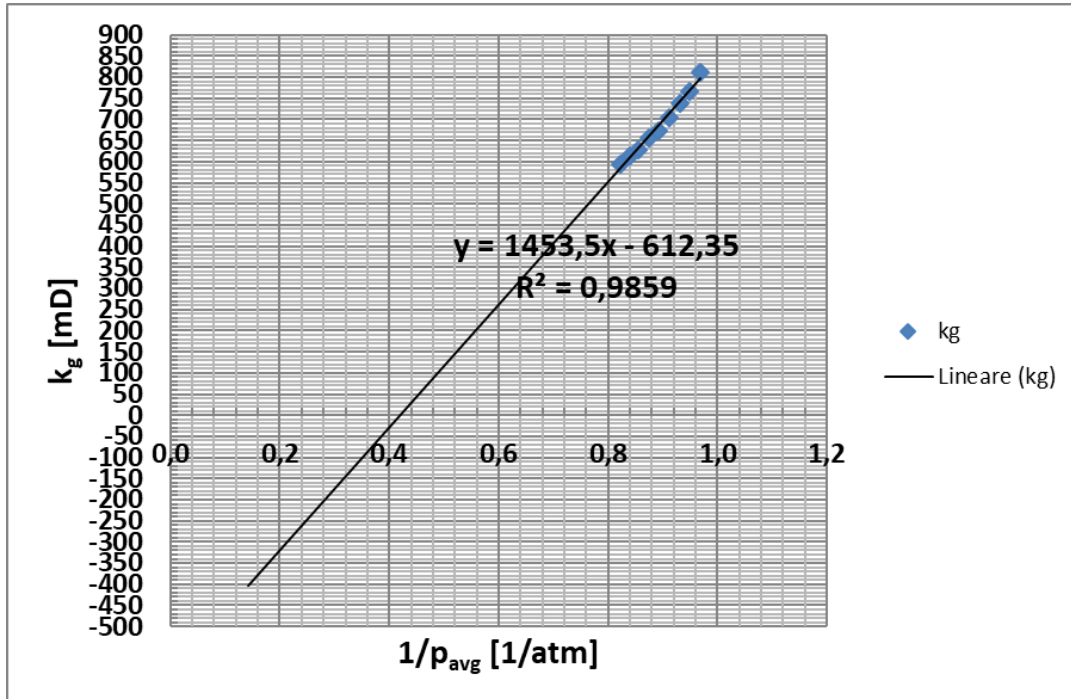


Figure 10- Linear Regression

What you retrieve from a laboratory analysis when you flow the core sample with one single fluid is the absolute permeability. The trend below is obtained from the correlation among the properties found by linear regression 2 (Table 31). In the y-axis, it is present  $\frac{p_1^2 - p_a^2}{q_g}$  and in the x-axis, it is the gas flow rate value,  $q_g$ , [ $\text{cm}^3/\text{s}$ ].

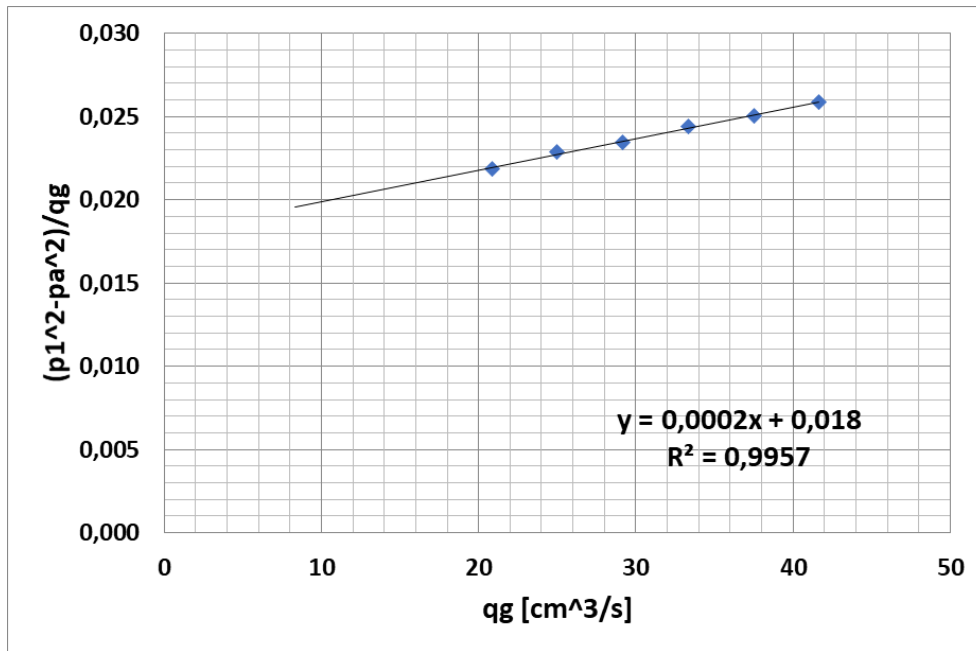


Figure 11- Absolute Permeability trend

As it is possible to see from the Fig.11, the trend shows a value of  $R^2$  very close to the unity, therefore it can be said that a good fitting is reached for the absolute permeability trend.

### 3.4 Klinkenberg effect

In the measurement of permeability is taken into account one assumption related to pressure value, which is considered so low that the gas behavior can be approximated to the one of an ideal gas. Therefore, a linear relationship is seen between the reciprocal pressure and the permeability under steady state condition and laminar flow. Anyway, it was observed that  $k$  changes with the gas pressure, explanation given by Klinkenberg who put his name to the phenomenon: the well known, Klinkenberg's effect (Kantzas A., *Fundamentals of Fluid Flow in Porous Media*; Klinkenberg L.J., *The Permeability of Porous Media to Liquids and Gases*).

In fact, Klinkenberg has discovered the existence of a thin layer, the so called Knudsen layer, thinner than the molecular mean free path, adjacent to the pore's wall where only molecules-wall collisions would occur and collisions among molecules could be ignored.

The slippage velocity captures the contribution of molecule-wall interactions and when this velocity is zero, the Poiseuille velocity profile (which results from molecule-molecule interaction) is recovered (Wikipedia).

Klinkenberg calibration is needed since to get a value of permeability equivalent to the permeability at formation condition you can incur in some problems (Lenormand R., *Permeability Measurement on Small Rock Samples*).

In addition, the phenomenon of gas slippage occurs during measurement because  $N_2$  is injected quickly from probe to core and it is very difficult to get an equilibrium in such short time (Wikipedia; Klinkenberg L.J., *The Permeability of Porous Media to Liquids and Gases*). Here, it is the formula, (6), to use in order to get rid of this problem:

$$k_g = k_l \left( 1 + \frac{b}{p} \right) \quad (6)$$

Where,

- $k_g$  is the permeability to gas, [mD];
- $k_l$  is the permeability to fluid, [mD];
- $b$  is the constant defined for a particular gas in a given rock type, [1/ mD \* atm];
- $p$  is the mean flowing pressure, [atm].

In general, it is assumed for  $b_{helium} = 44,6 (k / \phi)^{-0,447}$  and for  $b_{air} = 0,35b_{helium}$ .

So, for Klinkenberg  $k_{air}$  is always  $> k_{liquid}$ .

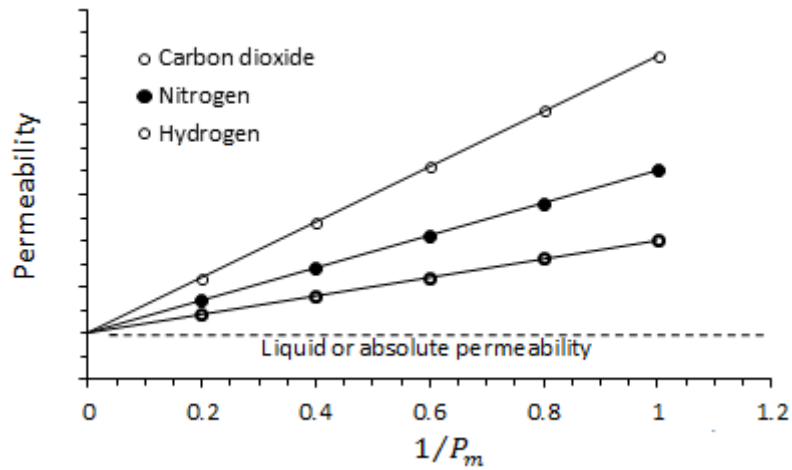


Figure 12- Klinkenberg effect case study: Permeability of Core Sample to Three Different Gases and Different Mean Pressure (Kantzas A., *Foundamentals of Fluid Flow in Porous Media*)

So, to get the permeability from the measurement of gas permeameter it is important to measure  $k$  for different pressure levels in order to know the relationship for the given core sample, which will be useful in the VBA program.

### 3.5 VBA coding programming

The coding program Visual Basic for Application with Excel is used here to get the permeability values in an easy way. It finds its applicability in many sectors, for creating macros, initiating a variable, executing a code line if a specific condition is met, and many others.

The reason why it was chosen is simply because it helps to reduce the work and moreover to get easily achieving the goal.

Besides, the program reads all the info necessary for the calculation of permeability, working on core geometry, lab pressure and temperature, flow rates and pressure levels corresponding to the rates (voltage changed into pressure values).

The Visual Basic for Application calculates  $k$  for each pressure step with the application of Darcy's law: this will result in multiple k-p point pairs.

Those values will be then subjected to a linear regression which will give three results: intersection, slope and  $R^2$ , according to a generic formula like that:

$$k(p) = k + \frac{k * b}{p} \quad (7)$$

Where,

- $k(p)$ : is the permeability to gas referred to the pressure level, [mD];
- $k$ : is the permeability to fluid, [mD];
- $b$ : is the specific constant for the gas type used, [1/ mD\* atm];
- $p$ : the mean flowing pressure, [atm].

$R^2$  is the quality of the fitting, obtained from the linear regression. When close to 1, it is possible to affirm that a good fitting has been reached: in all the cases of this analysis,  $R$  is very close to the unit.

In the following tables, it is possible to understand which data were used in order to get the result of permeability value for each core taken into this analysis.

Table 32- The measured permeability for sample A1

Sample				
A1				
Basic		$q_g$ [l/h]	Voltage [V]	Results
$d_1$ [cm]	3,805	20	1,058	$k$ [mD]= <b>-851</b>
$d_2$ [cm]	3,2	30	1,083	
$d_3$ [cm]	3,6	40	1,108	
$L_1$ [cm]	6,2	50	1,135	$b$ = <b>1994</b>
$L_2$ [cm]	6	60	1,163	
$L_3$ [cm]	5,8	70	1,189	
$T_a$ [°C]	24	80	1,218	$R^2$ = <b>0,99</b>
$P_a$ [bar]	1,007	90	1,245	
$V_0$ [V]	1,013	100	1,274	

Table 33- The measured permeability for sample A2

<b>Sample A2</b>					
<b>Basic</b>		<b>q<sub>g</sub> [l/h]</b>	<b>Voltage [V]</b>	<b>Results</b>	
<b>d<sub>1</sub> [cm]</b>	3,785	20	1,074	<b>k [mD]= -504,99</b>	
<b>d<sub>2</sub> [cm]</b>	3,218	30	1,11		
<b>d<sub>3</sub> [cm]</b>	3,799	40	1,147		
<b>L<sub>1</sub> [cm]</b>	5,128	50	1,185	<b>b= 1198,21</b>	
<b>L<sub>2</sub> [cm]</b>	5,153	60	1,226		
<b>L<sub>3</sub> [cm]</b>	5,119	70	1,265		
<b>T<sub>a</sub> [°C]</b>	24	80	1,31	<b>R<sup>2</sup>= 0,98</b>	
<b>P<sub>a</sub> [bar]</b>	1,007	90	1,353		
<b>V<sub>0</sub> [V]</b>	1,013	100	1,395		

Table 34- The measured permeability for sample 1B

<b>Sample 1B</b>					
<b>Basic</b>		<b>q<sub>g</sub> [l/h]</b>	<b>Voltage [V]</b>	<b>Results</b>	
<b>d1 [cm]</b>	3,818	20	1,037	<b>k [mD]= -3094</b>	
<b>d2 [cm]</b>	3,829	30	1,052		
<b>d3 [cm]</b>	3,792	40	1,065		
<b>L1 [cm]</b>	5,0321	50	1,083	<b>b= 4590</b>	
<b>L2 [cm]</b>	5,061	60	1,101		
<b>L3 [cm]</b>	5,036	70	1,117		
<b>T<sub>a</sub> [°C]</b>	24	80	1,133	<b>R<sup>2</sup> 0,95</b>	
<b>P<sub>a</sub> [bar]</b>	1,007	90	1,15		
<b>V<sub>0</sub> [V]</b>	1,013	100	1,17		

Table 35- The measured permeability for sample 2C

<b>Sample 2C</b>					
<b>Basic</b>		<b>q<sub>g</sub> [l/h]</b>	<b>Voltage [V]</b>	<b>Results</b>	
<b>d1 [cm]</b>	3,737	20	1,153	<b>k [mD]= 56,44</b>	
<b>d2 [cm]</b>	3,777	30	1,225		
<b>d3 [cm]</b>	3,756	40	1,291		
<b>L1 [cm]</b>	5	50	1,355	<b>b= 206,07</b>	
<b>L2 [cm]</b>	4,93	60	1,419		
<b>L3 [cm]</b>	4,999	70	1,481		
<b>T<sub>a</sub> [°C]</b>	24	80	1,541	<b>R<sup>2</sup> 0,99</b>	
<b>P<sub>a</sub> [bar]</b>	1,007	90	1,603		
<b>V<sub>0</sub> [V]</b>	1,013	100	1,662		

Table 36- The measured permeability for sample 2D

<b>Sample</b>					
<b>2D</b>					
<b>Basic</b>		<b>qg [l/h]</b>	<b>Voltage [V]</b>	<b>Results</b>	
<b>d1 [cm]</b>	3,916	20	1,067	<b>k [mD]=</b>	<b>-339,6</b>
<b>d2 [cm]</b>	3,938	30	1,104		
<b>d3 [cm]</b>	3,888	40	1,136		
<b>L1 [cm]</b>	4,647	50	1,167	<b>b=</b>	<b>915,92</b>
<b>L2 [cm]</b>	4,646	60	1,2		
<b>L3 [cm]</b>	4,624	70	1,235		
<b>Ta [°C]</b>	24	80	1,267	<b>R<sup>2</sup></b>	<b>0,92</b>
<b>Pa [bar]</b>	1,007	90	1,301		
<b>V0 [V]</b>	1,013	100	1,337		

Table 37- The measured permeability for sample 3D

<b>Sample</b>					
<b>3D</b>					
<b>Basic</b>		<b>qg [l/h]</b>	<b>Voltage [V]</b>	<b>Results</b>	
<b>d1 [cm]</b>	3,945	20	1,081	<b>k [mD]=</b>	<b>-288,9</b>
<b>d2 [cm]</b>	3,944	30	1,118		
<b>d3 [cm]</b>	3,957	40	1,159		
<b>L1 [cm]</b>	4,462	50	1,195	<b>b=</b>	<b>753,6</b>
<b>L2 [cm]</b>	4,538	60	1,242		
<b>L3 [cm]</b>	4,58	70	1,287		
<b>Ta [°C]</b>	24	80	1,335	<b>R<sup>2</sup></b>	<b>0,99</b>
<b>Pa [bar]</b>	1,007	90	1,381		
<b>V0 [V]</b>	1,013	100	1,424		

Table 38- The measured permeability for sample 1E

<b>Sample</b>					
<b>1E</b>					
<b>Basic</b>		<b>qg [l/h]</b>	<b>Voltage [V]</b>	<b>Results</b>	
<b>d1 [cm]</b>	3,926	20	1,257	<b>k [mD]=</b>	<b>14,1</b>
<b>d2 [cm]</b>	3,97	30	1,386		
<b>d3 [cm]</b>	3,936	40	1,505		
<b>L1 [cm]</b>	4,588	50	1,62	<b>b=</b>	<b>110,9</b>
<b>L2 [cm]</b>	4,584	60	1,735		
<b>L3 [cm]</b>	4,585	70	1,838		
<b>Ta [°C]</b>	24	80	1,942	<b>R<sup>2</sup></b>	<b>0,99</b>
<b>Pa [bar]</b>	1,007	90	2,048		
<b>V0 [V]</b>	1,013	100	2,152		

Table 39- The measured permeability for sample 2E

<b>Sample</b>					
<b>2E</b>					
<b>Basic</b>		<b>qg [l/h]</b>	<b>Voltage [V]</b>	<b>Results</b>	
<b>d1 [cm]</b>	3,927	20	1,195	<b>k [mD]=</b>	<b>16,11</b>
<b>d2 [cm]</b>	3,985	30	1,288		
<b>d3 [cm]</b>	3,999	40	1,372		
<b>L1 [cm]</b>	4,559	50	1,453	<b>b=</b>	<b>151,8</b>
<b>L2 [cm]</b>	4,544	60	1,542		
<b>L3 [cm]</b>	4,494	70	1,62		
<b>Ta [°C]</b>	24	80	1,702	<b>R<sup>2</sup></b>	<b>0,99</b>
<b>Pa [bar]</b>	1,007	90	1,807		
<b>V0 [V]</b>	1,013	100	1,889		

Table 39- The measured permeability for sample 3E

<b>Sample</b>					
<b>3E</b>					
<b>Basic</b>		<b>qg [l/h]</b>	<b>Voltage [V]</b>	<b>Results</b>	
<b>d1 [cm]</b>	3,942	20	1,162	<b>k [mD]=</b>	<b>59,43</b>
<b>d2 [cm]</b>	3,962	30	1,235		
<b>d3 [cm]</b>	3,941	40	1,304		
<b>L1 [cm]</b>	4,513	50	1,368	<b>b=</b>	<b>138,9</b>
<b>L2 [cm]</b>	4,427	60	1,437		
<b>L3 [cm]</b>	4,38	70	1,498		
<b>Ta [°C]</b>	24	80	1,556	<b>R<sup>2</sup></b>	<b>1,00</b>
<b>Pa [bar]</b>	1,007	90	1,621		
<b>V0 [V]</b>	1,013	100	1,678		

Table 40- The measured permeability for sample F1

<b>Sample</b>					
<b>F1</b>					
<b>Basic</b>		<b>qg [l/h]</b>	<b>Voltage [V]</b>	<b>Results</b>	
<b>d1 [cm]</b>	3,958	20	1,04	<b>k [mD]=</b>	<b>-2062,8</b>
<b>d2 [cm]</b>	3,968	30	1,056		
<b>d3 [cm]</b>	3,94	40	1,072		
<b>L1 [cm]</b>	4,609	50	1,089	<b>b=</b>	<b>3224,2</b>
<b>L2 [cm]</b>	4,686	60	1,108		
<b>L3 [cm]</b>	4,711	70	1,126		
<b>Ta [°C]</b>	24	80	1,146	<b>R<sup>2</sup></b>	<b>0,98</b>
<b>Pa [bar]</b>	1,007	90	1,166		
<b>V0 [V]</b>	1,013	100	1,187		

Table 41- The measured permeability for sample F2

<b>Sample</b>					
<b>F2</b>					
<b>Basic</b>		<b>qg [l/h]</b>	<b>Voltage [V]</b>	<b>Results</b>	
<b>d1 [cm]</b>	3,881	20	1,05	<b>k [mD]=</b>	<b>-934</b>
<b>d2 [cm]</b>	3,923	30	1,071		
<b>d3 [cm]</b>	3,901	40	1,093		
<b>L1 [cm]</b>	4,605	50	1,115	<b>b=</b>	<b>1811</b>
<b>L2 [cm]</b>	4,632	60	1,139		
<b>L3 [cm]</b>	4,683	70	1,161		
<b>Ta [°C]</b>	24	80	1,187	<b>R<sup>2</sup></b>	<b>0,98</b>
<b>Pa [bar]</b>	1,007	90	1,211		
<b>V0 [V]</b>	1,013	100	1,237		

Table 42- The measured permeability for sample G1

<b>Sample</b>					
<b>G1</b>					
<b>Basic</b>		<b>qg [l/h]</b>	<b>Voltage [V]</b>	<b>Results</b>	
<b>d1 [cm]</b>	3,779	20	1,445	<b>k [mD]=</b>	<b>38,89</b>
<b>d2 [cm]</b>	3,815	30	1,625		
<b>d3 [cm]</b>	3,802	40	1,772		
<b>L1 [cm]</b>	5,045	50	1,92	<b>b=</b>	<b>34,51</b>
<b>L2 [cm]</b>	4,993	60	2,06		
<b>L3 [cm]</b>	4,993	70	2,19		
<b>Ta [°C]</b>	24	80	2,305	<b>R<sup>2</sup></b>	<b>0,98</b>
<b>Pa [bar]</b>	1,007	90	2,433		
<b>V0 [V]</b>	1,013	100	2,552		

Table 43- The measured permeability for sample G2

<b>Sample</b>					
<b>G2</b>					
<b>Basic</b>		<b>qg [l/h]</b>	<b>Voltage [V]</b>	<b>Results</b>	
<b>d1 [cm]</b>	3,811	20	1,077	<b>k [mD]=</b>	<b>-540,16</b>
<b>d2 [cm]</b>	3,804	30	1,121		
<b>d3 [cm]</b>	3,794	40	1,167		
<b>L1 [cm]</b>	4,681	50	1,218	<b>b=</b>	<b>1072,0</b>
<b>L2 [cm]</b>	4,736	60	1,279		
<b>L3 [cm]</b>	4,802	70	1,344		
<b>Ta [°C]</b>	24	80	1,4	<b>R<sup>2</sup></b>	<b>0,96</b>
<b>Pa [bar]</b>	1,007	90	1,469		
<b>V0 [V]</b>	1,013	100	1,528		

Table 44- The measured permeability for sample G3

Sample					
G3					
Basic		qg [l/h]	Voltage [V]	Results	
d1 [cm]	3,77	20	1,202	k [mD]=	0,5
d2 [cm]	3,774	30	1,321		
d3 [cm]	3,762	40	1,424		
L1 [cm]	4,426	50	1,509	b=	168,7
L2 [cm]	4,448	60	1,608		
L3 [cm]	4,374	70	1,699		
Ta [°C]	24	80	1,795	R <sup>2</sup>	0,96
Pa [bar]	1,007	90	1,893		
V0 [V]	1,013	100	1,988		

Table 45- The measured permeability for sample H2

Sample					
H2					
Basic		qg [l/h]	Voltage [V]	Results	
d1 [cm]	3,78	20	1,046	k [mD]=	-1676
d2 [cm]	3,744	30	1,066		
d3 [cm]	3,726	40	1,085		
L1 [cm]	5,243	50	1,104	b=	2865
L2 [cm]	5,237	60	1,13		
L3 [cm]	5,186	70	1,152		
Ta [°C]	24	80	1,175	R <sup>2</sup>	0,97
Pa [bar]	1,007	90	1,199		
V0 [V]	1,013	100	1,222		

Table 46- The measured permeability for sample H4

Sample					
H4					
Basic		qg [l/h]	Voltage [V]	Results	
d1 [cm]	3,78	20	1,046	k [mD]=	-1676,5
d2 [cm]	3,744	30	1,066		
d3 [cm]	3,726	40	1,085		
L1 [cm]	5,243	50	1,104	b=	2864,95
L2 [cm]	5,237	60	1,13		
L3 [cm]	5,186	70	1,152		
Ta [°C]	24	80	1,175	R <sup>2</sup>	0,97
Pa [bar]	1,007	90	1,199		
V0 [V]	1,013	100	1,222		

The values of permeability obtained with the program are a bit different for the different samples, and this can be explained taking into account the different size distribution.

In addition, the presence of possible fractures inside in specimens or undesired void spaces may alter the value of expected  $k$ .

So, to get a positive value of permeability you can also apply the formula (7) and have the following values of  $k$ :

Table 47- The measured permeability for atmospheric pressure

Sample	$k$ [mD]	$k*b$ [1/mD*atm]	$k$ [ p <sub>atm</sub> ]
A1	-851	1994	1143
A2	-504,99	1198,21	693,22
A3	19,73	207,21	226,94
1B	-3094	4509	1415
2C	56,44	206,07	262,51
2D	-339,6	915,92	576,32
3D	-288,9	753,6	464,7
1E	14,1	110,9	125
2E	16,11	151,8	167,91
3E	59,43	138,9	198,33
F1	-2062,8	3224,2	1161,4
F2	-934	1811	877
G1	38,89	34,51	73,4
G2	-540,16	1072	531,84
G3	0,5	168,7	169,2
H2	-1676	2865	1189
H4	-1676,5	2864,95	1188,45

### 3.6 The *calculated permeability*

The above paragraph deals with the measurements of permeability for specimens realized artificially in laboratory. Under lab conditions we assume: laminar flow and Darcy's law applicability.

Two conditions that not always can be considered valid, especially when you need to consider the presence of fractures inside the core samples and their influence on them.

A new recent method was developed to calculate permeability of a porous medium with microfractures.

The idea behind of this study is to consider the permeability of one fracture and then to determine the equivalent permeability of the whole system, called "apparent permeability", as in the case of apparent resistivity in parallel connection (Pasztor A., *Method To Analyze the Effect of Fractures in Tight Reservoir*; Pasztor A., *Method To Calculate Apparent Permeability of Hydraulic Fractures*; Pasztor A., *Effect of Microfractures on Filtration*).

$$k_a = \frac{k_m A_m + \sum k_f A_f}{A_s} \quad (8)$$

Where:

- $k_a$  is the apparent permeability of the system [mD];
- $k_m$  and  $A_m$  are the permeability [mD] and cross-sectional area [m<sup>2</sup>] of the matrix;
- $k_f$  and  $A_f$  are the equivalent permeability[mD] and cross-sectional area [m<sup>2</sup>] of one fracture;
- $A_s$  is the cross-sectional area [m<sup>2</sup>] of the system.

The equivalent permeability of one channel can be calculated from its radius as follows (Pasztor A., *Method To Calculate Apparent Permeability of Hydraulic Fractures*):

$$k_f = \frac{r_f^2}{8} 10^{15} \quad (9)$$

Where:

- $k_f$  is the equivalent permeability [mD] of one fracture;
- $r_f$  is radius of the fracture, [m].

From this radius we will retrieve the  $k_r$ , resultant permeability of the whole system, by using this formula:

$$k_r = \frac{A_f * k_f}{A_s} \quad (10)$$

In which:

- $k_r$  is the resultant permeability of the system, [mD];
- $k_f$  and  $A_f$  are the equivalent permeability [mD] and cross-sectional area [m<sup>2</sup>] of one fracture;
- $A_s$  is the cross-sectional area [m<sup>2</sup>] of the system.

But by definition,

$$\varphi = \frac{V_p}{V_t} = \frac{A_p * l}{A_t * l} = \frac{A_f}{A_s} \quad (11)$$

Where:

- $\varphi$  is porosity, [-];
- $V_p$  is the pore volume, [m<sup>3</sup>];
- $V_t$  is the total volume, [m<sup>3</sup>];
- $A_p$  is the area of the pores, [m<sup>2</sup>];
- $A_t$  is the total cross-sectional area of the system, [m<sup>2</sup>];
- $l$  is the length, [m];
- $A_f$  is the cross-sectional area of one fracture, [m<sup>2</sup>];
- $A_s$  is the cross-sectional area [m<sup>2</sup>] of the system.

You can consider that the ratio between the area of a single fracture, represented by a channel, and the total area, i.e. the area of the whole system, is by definition the value of porosity.

Therefore, you can rewrite the equation for  $k$  as follows:

$$k_r = \varphi * k_f \quad (12)$$

Where,

- $k_r$  is the resultant permeability of the system, [mD];
- $\varphi$  is porosity, [-];
- $k_f$  is the equivalent permeability of one fracture, [mD].

To be more precise, we can divide this value of  $k_r$  by tortuosity because in reality it is almost impossible to find straight channel in the configuration of grains.

So, to obtain a more realistic value you will use also the Comiti and Renaud method for monosized sphere (Passtor A., *Method To Calculate Apparent Permeability of Hydraulic Fractures*):

$$\tau = 1 - 0,4 \ln(\varphi) \quad (13)$$

Where,

- $\tau$  is tortuosity value, [-];
- $\phi$  is the same it was used before, [-].

To reach the final result of the calculated permeability, it is also required to consider the mean particle radius,  $R$ .

This value is obtained by some simple calculations:

$$R = \frac{\left\{ \text{sum} \left[ x \left( \frac{f(x)}{100} \right) \right] \right\}}{2} \quad (14)$$

Where,

- $x$  is the size distribution;
- $f(x)$  is the fraction in mass percentage present in that range analyzed.

### 3.7 Geometrical considerations

It is also important to underline the role of geometry in this situation. In fact, you can distinguish two configurations: an ideal and a tetrahedral geometry (Fig13 and Fig.14) (Pasztor A., *Method To Calculate Apparent Permeability of Hydraulic Fractures*).

The first one is closer to our case due to the fact that the compression given while realizing the cores was not so much high to reach the possibility to fulfil all the space grain to grain. So, the void space in this case results as the greatest with biggest channels radius and higher permeability.

The other case is when the void space is the lowest and therefore, the radius of the channels the smallest, but the k value the more realistic.

Both configurations look like (Pasztor A., *Method To Calculate Apparent Permeability of Hydraulic Fractures*):

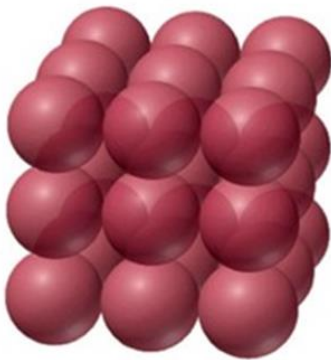


Figure 13- Ideal geometry

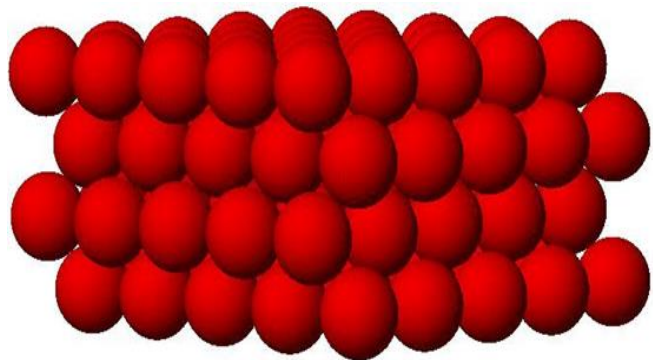


Figure 14- The tetrahedron

The ideal situation seems to be impossible to exist in reality because the compacting effect of the closure pressure cannot make a configuration like that. Moreover, the calculation of permeability will be overestimated and the channel radius will consider the distance between layers.

Indeed, as a correction we assume the radius of the conductive channels to be the same as the radius of the pore throats in the system.

That means in terms of graphic representation (Pasztor A., *Method To Calculate Apparent Permeability of Hydraulic Fractures*) :

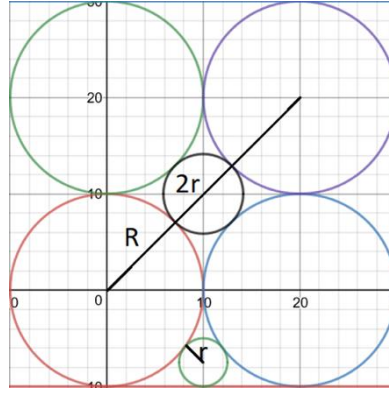


Figure 15- Channel radius for ideal geometry

Where radius of channel between layers can be calculated as (Pasztor A., *Apparent Permeability of Fractures*):

$$2r_l = \sqrt{(2R)^2 + (2R)^2} - 2R \quad (15)$$

$$r_l = R(\sqrt{2} - 1) \quad (16)$$

And the channel radius between formation and layer is equal to:

$$r_f = \frac{R}{4} \quad (17)$$

In which,

- $r_l$  is the inner radius for the layer, [m];
- $r_f$  is the radius next to the formation, [m];
- $R$  is the radius between the sphere, [m].

By knowing the radius, it is also possible to retrieve an exact value of porosity that can be used with a different number for the configurations mentioned above. See the formula (Pasztor A., *Method To Calculate Apparent Permeability of Hydraulic Fractures*):

$$\varphi_0 = \frac{V_p}{V_s} = \frac{V_b - V_s}{V_b} = \frac{d^3 - \frac{d^3\pi}{6}}{d^3} = 1 - \frac{\pi}{6} = 0,4764 \quad (18)$$

In the case of tetrahedral geometry the calculation of the radius, in particular that one between formation and layer, follows the same trend, according to a new complex geometry of the system (the tetrahedron), while the inner radius of the layer does not change that much.

So, the porosity is calculated by considering this new configuration:

$$\phi_0 = \frac{V_p}{V_s} = \frac{V_b - V_s}{V_b} = \frac{\frac{d^3}{\sqrt{2}} - \frac{d^3\pi}{6}}{\frac{d^3}{\sqrt{2}}} = 1 - \frac{\pi\sqrt{2}}{6} = 0,25951 \quad (19)$$

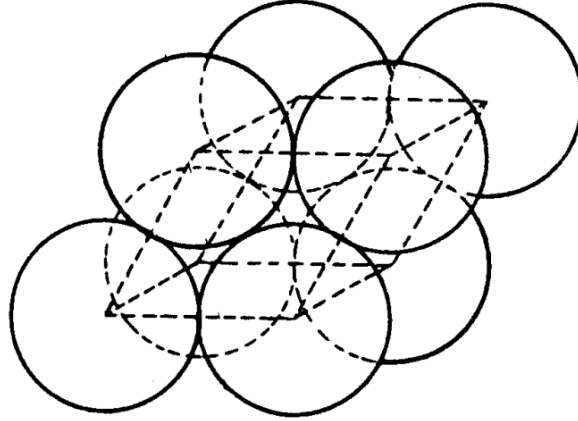


Figure 16 The tetrahedron configuration

The centers of 4 spheres create a tetrahedron, which consists of 4 pieces of 1/8 sphere and 4 pieces of 1/2 channels. By approximating a uniform channel for the radius, you can come to this solution:

$$\phi_0 \times 4 \times \frac{1}{8} \times \frac{4}{3} R^3 \pi = 4 \times \frac{1}{2} \times R \times r_l^2 \pi \quad (20)$$

$$r_l = R \sqrt{\frac{\phi_0}{3}} \quad (21)$$

#### TETRAHEDRAL GEOMETRY

From the particle size distribution, analyzed with laser scattering (as seen in chapt.2), the size values were multiplied by the fractions and then calculating the mean radius dividing by 2 what obtained from the sum of the values used (Pasztor A., *Method To Calculate Apparent Permeability of Hydraulic Fractures*).

After that, the channel radius has been calculated applying the formula coming from the equilibrium equation, (20), for the tetrahedron's volume:

$$r_{ch} = R * \sqrt{\frac{\phi_0}{3}} \quad (22)$$

Where,

- $r_{ch}$  is the channel radius, [m]:

- $R$  is the mean radius from the particle size distribution, [m];
- $\varphi$  is porosity (a given value equal to 0,26 for this case), [-].

By knowing the channel radius, it is possible to calculate the channel permeability, simply applying the following:

$$k_{ch} = \frac{r_{ch}^2}{8} \quad (23)$$

- $k_{ch}$  is the channel permeability, that means for one channel only.

Then, knowing permeability to one channel it is possible to calculate permeability of the system by considering this:

$$k_{resultant} = \frac{A_{ch} * k_{ch}}{A_s} \quad (24)$$

In which,

- $k_{resultant}$  is permeability to the system (sample), [mD];
- $A_{ch}$  is the area of one single channel, [m<sup>2</sup>];
- $k_{ch}$  is permeability to one channel, [mD];
- $A_s$  the area of the system “core”, [m<sup>2</sup>].

But you can also rewrite the above formula, taking into account that:

$$A = \frac{V_{ch}}{V_s} = \frac{A_{ch} * l}{A_s * l} = \frac{A_{ch}}{A_s} \quad (25)$$

By definition of porosity, you can write that:

$$\varphi = \frac{V_p}{V_t} = \frac{V_{ch}}{V_s} \quad (26)$$

Which is to say,

$$\varphi = \frac{A_{ch}}{A_s} \quad (27)$$

Where,

- $V_{ch}$  is the volume of one channel, [m<sup>3</sup>];

- $V_s$  is the volume of the system, [m<sup>3</sup>];
- $V_p$  is the pore volume, [m<sup>3</sup>];
- $V_t$  is the total volume (system), [m<sup>3</sup>].

Therefore,

$$k_{resultant} = k_{ch} * \varphi \quad (28)$$

Which is the porosity calculated before: so, for tetrahedron  $\varphi = 0,26$  and for the ideal geometry  $\varphi = 0,475$  (Pasztor A., *Method To Calculate Apparent Permeability of Hydraulic Fractures*).

In addition, to decrease the value of the resultant permeability you need to take into account the tortuosity effect. That's why you have to calculate:

$$\tau = 1 - 0,4\varphi \quad (29)$$

In which,

- $\tau$  is the tortuosity, [-];
- $\Phi$  is the same porosity considered above, [-].

Then, you have to divide the value of the resultant permeability by  $\tau$ , and all the values can be read in the table below, (Table 48).

Table 48- Results

SERIES A							
R mean [m]	r channel	$\phi$ [-]	k channel [m]	k resultant	$\tau$ [-]	kr corrected	kr [mD]
0,0000506	5,11E-06	0,26	3,3E-12	8,5E-13	0,896	7,6E-13	8E+02

$$k_r = 800 \text{ mD}$$

The corrected permeability reported above shows a higher value, which is good in terms of reservoir engineering field, and it can be justified, for instance, because of the presence of big grains with noticeable interstitial space between them.

#### IDEAL GEOMETRY

Same procedure is followed in this case, but different will be the result of the permeability since as already discussed, this is a situation on which  $k$  tends to be overestimated because it is hard to find in reality such an easy configuration, that seems so perfect especially for the compaction point of view!

Table 49- Results of calculations for Ideal Geometry case

SERIES A							
R mean [m]	r channel	$\phi$ [-]	k channel [m]	k resultant	$\tau$ [-]	kr corrected [	kr [mD]
0,00005	1,26E-05	0,475	1,99988E-11	9,499E-12	0,81	7,69454E-12	7695

$$k_r = 7695 \text{ mD}$$

As it is possible to observe there is a consistent different between the two values in the analyzed configurations. In the case of the specimens here created, because of lack compression applied, the configuration closer to our result will be the ideal geometry.

Now, the same it is repeated for the other series. Look at the tables below.

Table 50 - Results for series B

SERIES B - TETRAHEDRAL GEOMETRY							
R mean [m]	r channel	$\phi$ [-]	k channel [m]	k resultant	$\tau$ [-]	kr corrected [	kr [mD]
0,0000507	5,13E-06	0,26	3,3E-12	8,5E-13	0,896	7,7E-13	8E+02
SERIES B - IDEAL GEOMETRY							
R mean [m]	r channel	$\phi$ [-]	k channel [m]	k resultant	$\tau$ [-]	kr corrected [	kr [mD]
0,00005	1,27E-05	0,475	2,0112E-11	9,553E-12	0,81	7,7381E-12	7738

Table 51 - Results for series C

SERIES C - TETRAHEDRAL GEOMETRY							
R mean [m]	r channel	$\phi$ [-]	k channel [m]	k resultant	$\tau$ [-]	kr corrected [	kr [mD]
0,0000494	4,99E-06	0,26	3,1E-12	8,1E-13	0,896	7,3E-13	7E+02
SERIES C - IDEAL GEOMETRY							
R mean [m]	r channel	$\phi$ [-]	k channel [m]	k resultant	$\tau$ [-]	kr corrected [	kr [mD]
0,00005	1,23E-05	0,475	1,90598E-11	9,053E-12	0,81	7,33325E-12	7333

Table 52 - Results for series D

SERIES D - TETRAHEDRAL GEOMETRY							
R mean [m]	r channel	$\phi$ [-]	k channel [m]	k resultant	$\tau$ [-]	kr corrected [	kr [mD]
0,0000504	5,09E-06	0,26	3,2E-12	8,4E-13	0,896	7,6E-13	8E+02
SERIES D - IDEAL GEOMETRY							
R mean [m]	r channel	$\phi$ [-]	k channel [m]	k resultant	$\tau$ [-]	kr corrected [	kr [mD]
0,00005	1,26E-05	0,475	1,98492E-11	9,428E-12	0,81	7,63697E-12	7637

Table 53 - Results for series E

SERIES E - TETRAHEDRAL GEOMETRY							
R mean [m]	r channel	$\phi$ [-]	k channel [m]	k resultant	$\tau$ [-]	kr corrected [	kr [mD]
0,0000495	5E-06	0,26	3,1E-12	8,1E-13	0,896	7,3E-13	7E+02
SERIES E - IDEAL GEOMETRY							
R mean [m]	r channel	$\phi$ [-]	k channel [m]	k resultant	$\tau$ [-]	kr corrected [	kr [mD]
0,00005	1,24E-05	0,475	1,91153E-11	9,08E-12	0,81	7,35462E-12	7355

Table 54 - Results for series F

SERIES F - TETRAHEDRAL GEOMETRY							
R mean [m]	r channel	$\phi$ [-]	k channel [m]	k resultant	$\tau$ [-]	kr corrected	kr [mD]
0,0000505	5,1E-06	0,26	3,3E-12	8,5E-13	0,896	7,6E-13	8E+02
SERIES F - IDEAL GEOMETRY							
R mean [m]	r channel	$\phi$ [-]	k channel [m]	k resultant	$\tau$ [-]	kr corrected	kr [mD]
0,00005	1,26E-05	0,475	1,99239E-11	9,464E-12	0,81	7,66573E-12	7666

Table 55 - Results for series G

SERIES G - TETRAHEDRAL GEOMETRY							
R mean [m]	r channel	$\phi$ [-]	k channel [m]	k resultant	$\tau$ [-]	kr corrected	kr [mD]
0,0000497	5,02E-06	0,26	3,2E-12	8,2E-13	0,896	7,4E-13	7E+02
SERIES G - IDEAL GEOMETRY							
R mean [m]	r channel	$\phi$ [-]	k channel [m]	k resultant	$\tau$ [-]	kr corrected	kr [mD]
0,00005	1,24E-05	0,475	1,93097E-11	9,172E-12	0,81	7,42939E-12	7429

Table 56 - Results for series H

SERIES H - TETRAHEDRAL GEOMETRY							
R mean [m]	r channel	$\phi$ [-]	k channel [m]	k resultant	$\tau$ [-]	kr corrected	kr [mD]
0,0000505	5,11E-06	0,26	3,3E-12	8,5E-13	0,896	7,6E-13	8E+02
SERIES H - IDEAL GEOMETRY							
R mean [m]	r channel	$\phi$ [-]	k channel [m]	k resultant	$\tau$ [-]	kr corrected	kr [mD]
0,00005	1,26E-05	0,475	1,99392E-11	9,471E-12	0,81	7,6716E-12	7672

The final results of permeability, both for tetrahedral geometry and ideal case, show values which seem to be inconsistent. The expected values should have been a bit different, but since it is a project work still on going, the obtained results are not seen as a failure because it may be due to some flaws during calculation or in the creation itself of the samples. Anyway, the method is approved and requires more work to be performed in time.

## FOURTH CHAPTER

### ***“CORRELATIONS AMONG THE PROPERTIES OF THE SPECIMENS”***

#### 4.1 *“Grain size distribution vs Permeability”*

As already said, grain size distribution represents one of the most important parameter that has been used to set specific characteristics in a rock: determining the filter pack, estimating the hydraulic conductivity, analyzing the geo-technical properties and also listing the oil reservoir characteristics. Moreover, it permits the subdivision of rock types in classes based on the particle dimensions (Gilbert, A. S., *Grain Size Analysis- Encyclopedia of Earth Science Series*; Griffiths, J.C., *Grain Size Distribution and Reservoir Rock Characteristics*; Jillavenkatesa A., *Particle Size Characterization*). Since in nature sediments are made as an amalgamation of several particle sizes, grain size has to be considered like a continuous variable. Particle or grain size is a fundamental attribute or physical property of particulate samples or sediments and sedimentary rocks (Wikipedia).

Sediment, soil, or material properties are directly influenced by the size of its particles, as well as their shape (form, roundness and surface texture or the grains) and fabric (grain-to-grain interrelation and grain orientation), such as texture and appearance, density, porosity, and permeability.

The size of particles is directly dependent on many features such as the environment of setting, the transport duration and agents, the depositional conditions, and moreover external factors on a local and regional area.

The size of the particles is defined by the nominal diameter, which can be expressed by millimeters, microns or phi units.

The influence of the grain size on rock properties is truly relevant since the particle size distribution is used as a straightforward method to easily get information for the estimation of permeability (Beard, D.C., *Influence of Texture on Porosity and Permeability of Unconsolidated Sand*; Oluveni G., *Prediction of Directional Grain Size Distribution: an Integrated Approach*; Pryor, W. A., *Permeability – Porosity Patterns and Variations in Some Holocene Sand Bodies*). But its role assumes importance also in relation to other properties that characterize the rock behavior.

In particular, it can be declared that permeability increases with grain size. This finds its explanation by taking the definition of permeability which is strictly connected to the amount of free space available for fluids to flow. So, if the fluid path is blocked due to poorly sorted rock sizes, the effect will be a limited fluid quantity flowing through the pores.

From the PSD analysis by using laser scattering method and with the help of software Grapher, it was possible to get a distribution values and a distribution curve for each samples series created in lab.

By considering the mean particle radius, which derives from the size distribution as well, (equation 14, chapt.3, paragraph 3.5), you can get a correlation that shows the relation between the two properties.

The correlation between R and k is shown below on the graph, Fig.17:

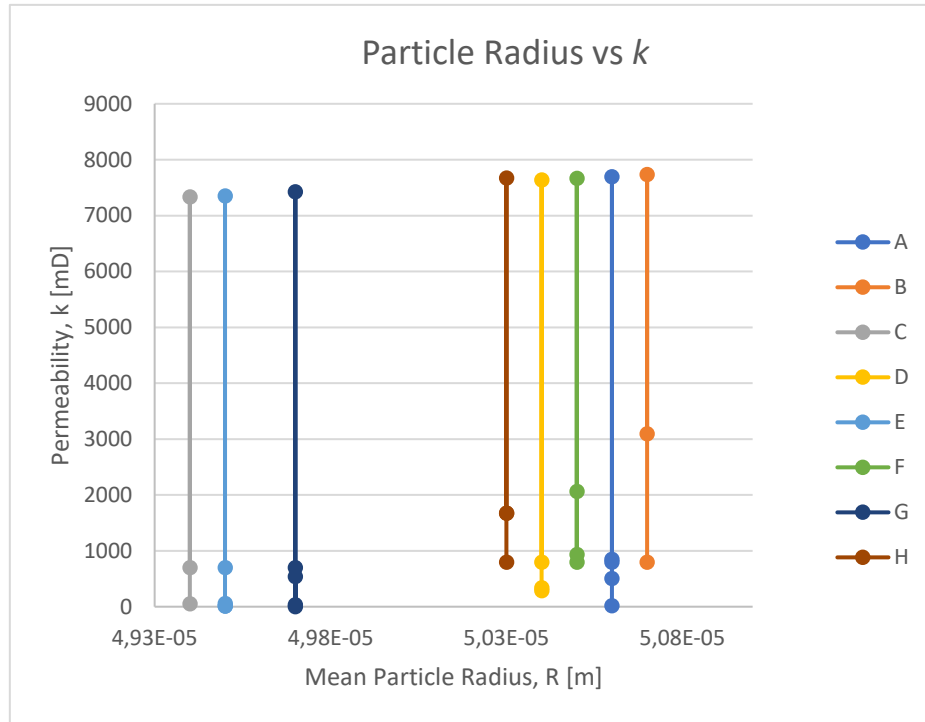


Figure 17 - Representation of R vs k

The graph shows the different behavior of the samples, each one characterized by a different distribution and different permeability values (here, the maximum value that means the overestimated value of k with the ideal geometry, the minimum value, which is the k calculated for tetrahedral configuration, and the values of measured permeability for the cores of the series).

From what it came out, it is possible to observe that series B shows the highest particle size distribution, even though it was made by 70% sand <sub>315</sub> and 30% sand <sub>500</sub> and if compared to other options, it should not be the largest value. This can explain by two possibilities: first, it may be present flaw during calculations; and second, the screening process was conducted by hands and therefore, it may causes the 315 type sand with high mean radius than others.

Anyway, to better analyze the graph you may need to remind the percentage of each fraction in every single series. So, here you go:

A: 50% fraction 500 – 50% fraction 315

B : 70% fraction 315 -30% fraction 500

C: 50% fraction 200 – 50% fraction <200

D: 50% fraction 315 – 50% fraction 200

E: 50% fraction 315 – 50% fraction <200

F: 70% fraction 500 – 30% fraction 315

G: 25% fraction <200 – 25% fraction 200 – 25% fraction 315 – 25% fraction 500

H: 35% fraction 315 – 65% fraction 500

It is consistent with what said about the relation between permeability and grain size distribution for series C, which is made by the lowest particles size. But for the others there is the same problem before analyzed.

The bonding existing between the two properties can be resumed as: coarser grain sediments are more permeable than fine- grained ones because the pores between grain particles are larger and therefore more fluid can be free to move inside. So, permeability increases as particle size increases too (Fukuda M., *Grain Size Distribution vs Coefficient of Permeability of Marine Clay*; Griffiths, J.C., *Grain Size Distribution and Reservoir Rock Characteristics*).

Other characteristics such as sorting, grain shape, packing and arrangement of particles take a considerable impact on permeability, as well as the cement bonding (you may see the results to understand better how all these properties are connected each others) (Milton M.W., *Effect of Grain Size, Grain Shape, and Clay Particle on Oil Recovery by Water Flooding*).

For sure, it can be said that knowing the grain size distribution you may be able to get a great contribution for the investigation of permeability of the entire porous system.

#### 4.2 Porosity and Particle Size Distribution

Soil retains fluid, that can be water, oil or gas (or mix of those) in the void spaces, formed in between particles. This amount of space in a soil sample defines its porosity, that is the storage capacity of that sediment. In order to investigate on the relation between porosity and particle size distribution, you better refresh the definition of porosity itself: it is in fact the ratio of pore volume to its total volume (Ogolo N. A., *Effects of Grain Size on Porosity Revisited*).

Porosity is surely controlled by grain size distribution, together with other characteristics which define a rock: cementation, diagenetic history, and composition. But at the same time porosity is not controlled by the grain size, in the sense that the space grain to grain is related only to the method of grain packing.

To see how grain size affects porosity you should take into account, for instance, poorly sorted sediments, in details those ones with a larger range of grain sizes: why? Because the finer particles tend to fill the spaces between the larger ones, resulting in lower porosity (due to lack of available space) (Arthy L.F., *Density, Porosity, and Compaction of Sedimentary Rocks*).

In fact it can be said that, the larger sized particles do not pack well once together, so they tend to show bigger spaces: which is to say more fluid can pass through in a quickly way too!, and more storage capacity they do show where the smaller grains go through and accumulate, creating a poorly sorted sediments (Wikipedia).

Graphically it can be shown below, in Fig.18: high porosity is registered by well sorted particles and low porosity is for poorly sorted soil, for the reasons already explained.

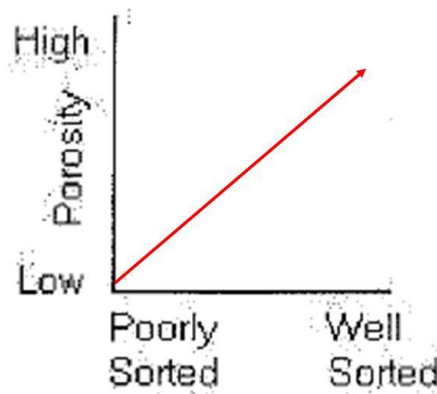


Figure 18 - Porosity vs Sorting (*Porosity vs Particle size*, encyclopedia.com The World of Earth and Science)

For a matter of fact, this is true for unconsolidated materials which are anyway affected by the arrangement and size, grain shape and packing method.

In reference to this works and the core samples made up, it is possible to observe the trend of porosity plot with the mean particle radius, below (Fig.19).

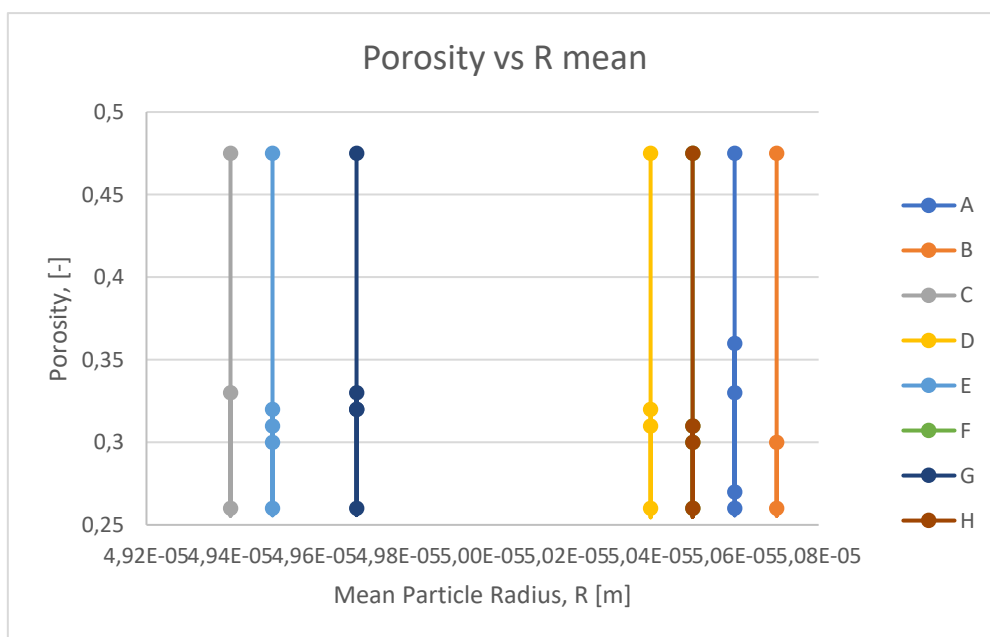


Figure 19 - Relation between Porosity and R

They show the same representation with permeability, probably because of some “mistakes” met during the elaboration of the data and mainly during the process of creation itself. Even here, you how the series B shows the highest values in grain size distribution with respect to others (maybe because they pack better than the other cores).

## ***CONCLUSION***

The possibility to create artificial cores, shown in this work, may represent a useful process to help investigating the rock properties at a low cost.

The idea of creating artificial sand specimens which show the same characteristics of the real ones can give a great opportunity to perform experimental work, especially when cores are not available or when analysis should be executed on cores with specific, large dimensions.

Petrophysical properties were measured on samples characterized by different grain size distributions. 40 cores were analysed to measure porosity and permeability; however, due to some errors and uncertainties affecting the final results a clear correlation between porosity and permeability versus grain size distribution could not be established.

Therefore, the reaserch outcome was in some way disappointing. Also, further investigations are required to explain the obtained results.

## REFERENCES

- Arthy, L. F., (1930), *Density, Porosity, and Compaction of Sedimentary Rocks*, Bull. Amer. Assoc. Petrol. Geol. Vol.
- Beard, D.C. and Weyl, P.K., *Influence of Texture on Porosity and Permeability of Unconsolidated Sand*. American Association of Petroleum Geologists Bull, 1973.
- Cipriani, N. (1996), *The Encyclopedia of Rocks and Minerals*. New York: Barnes&Noble.
- Dale, C.B., Macfarlane, R.M., and Hughes, R.V., (1950), *The Effect of Pore Size on Oil Recovery When Flooding Along Unconsolidated Sand Cores*.
- Faisal M., *Helium Porosimeter*, Project Thesis at Koya University.
- Fukuda M., (Osaka Soil Test Laboratory), *Grain Size Distribution vs Coefficient of Permeability of Marine Clay*, Major Effect of Grain Size Distribution. The 7<sup>th</sup> International Offshore and Polar Engineering Conference, 25-30 May, Honolulu, Hawaii, USA, 1997.
- Gilbert, A. S, and Lopez, G., *Grain Size Analysis- Encyclopedia of Earth Science Series, Encyclopedia of Geoarcheology*, Springer 2017.
- Griffiths, J.C., (1952), *Grain Size Distribution and Reservoir Rock Characteristics*, Bulletin of the American Association of Petroleum Geologists.
- Ishimwe, D., *Reservoir Rock Properties*, connect.spe.org, 2014.
- Jillavenkatesa, A., Dapkunas, S.J., Lin- Sien *Particle Size Characterization*, NIST Special Publication, 2001.
- Jishun Q., *The Manufacture and Use of Artificial Consolidated Core Samples in China*, Research Institute of Petroleum Exploration and Development, PetroChina.
- Kantzas, A., Bryan J., Taheri, S., *Fundamentals of Fluid Flow in Porous Media*.
- Klinkenberg, L.J., *The Permeability of Porous Media To Liquids and Gases*, Drilling and Production Practice, 1 Jan., New York, American Petroleum Institute.
- Lenormand, R., *Permeability Measurement on Small Rock Samples*.
- Mc Cave, I. N., Bryant, R. J., Cook, H.F., Coughanowr, C.A., (July 1986), *Evaluation of A Laser Diffraction Size Analyzer For Use with Natural Sediments*. Journal of Sedimentary Research.
- Milton, M.W., Laverty, T.R., Bystron, G.R., and Guerrero, E.T., *Effect of Grain Size, Grain Shape, and Clay Particle on Oil Recovery by Water Flooding*, SPE 247 University of Tuluse.
- Ogolo, N.A., (Institute of Petroleum Studies and Department of Petroleum and Gas Engineering, University of Portharcourt, River State, Nigeria). *Effects of Grain Size on Porosity Revisited*, SPE Nigeria Annual International Conference and Exhibition, 4-6 August, Lagos. Nigeria, 2015.
- Oluvemi, G. (Robert Gordon University), Ovenevian, B., MacLoad, C., *Predictions of Directional Grain Size Distribution: an Integrated Approach*. Nigeria Annual International Conference and Exhibition, 31 July – 2 August, Abuja, Nigeria, 2006.
- Pasztor, A. V., *Apparent Permeability of Fractures*, 6<sup>th</sup> Annual Student Energy Congress, ASEC 2019 Oil and Gas Tech., Zagreb, Croatia.
- Pasztor, A. V., Remeczki, F., *Effect of Microfractures on Filtration*, in 18<sup>th</sup> International Multidisciplinary Scientific Geoconference SGEM, Alberna, Bulgaria, 2018.
- Pasztor, A. V., *Method To Analyze The Effect of Fractures in Tight Reservoir*, University of Miskolc.
- Pasztor, A. V., Lengyel, T., *Method To Calculate Apparent Permeability of Hydraulic Fractures*. University of Miskolc, Hungary.
- Pryo, W. A., (1973), *Permeability . Porosity Patterns and Variations in Same Holocene Sand Bodies*, Journ., sed., Petrology.
- Selley, R. C., (2000), *Applied Sedimentology*, Second Edition Academic Press.
- [www.encyclopedia.com](http://www.encyclopedia.com), *Porosity and Permeability*, The World of Earth Science.
- [www.rigzone.com](http://www.rigzone.com), *How Does Core Analysis Work?*
- Wikipedia Source.